Physics of metabolic organization

Marko Jusup[a], Tânia Sousa[b], Tiago Domingos[b], Velimir Labinac[c], Nina Marn[d], Zhen Wang[e], Tin Klanjšček[d]

[a]*Center of Mathematics for Social Creativity, Hokkaido University*
5-8 Kita Ward, Sapporo 060-0808, Japan
[b]*Maretec, Instituto Superior Técnico, Universidade de Lisboa*
Av. Rovisco Pais 1, 1049-001 Lisboa, Portugal
[c]*Department of Physics, University of Rijeka*
R. Matejčić 2, 51000 Rijeka, Croatia
[d]*Department for Marine and Environmental Research, Rudjer Boskovic Institute*
Bijenička 54, 10000 Zagreb, Croatia
[e]*Interdisciplinary Graduate School of Engineering Sciences, Kyushu University*
6-1 Kasuga-koen, Kasuga, Fukuoka 816-8580, Japan

Abstract

We review the most comprehensive metabolic theory of life existing to date. A special focus is given to the thermodynamic roots of this theory and to implications that the laws of physics—such as the conservation of mass and energy—have on all life. Both the theoretical foundations and biological applications are covered. Hitherto, the foundations were more accessible to physicists or mathematicians, and the applications to biologists, causing a dichotomy in what always should have been a single body of work. To bridge the gap between the two aspects of the same theory, we (i) adhere to the theoretical formalism, (ii) try to minimize the amount of information that a reader needs to process, but also (iii) invoke examples from biology to motivate the introduction of new concepts and to justify the assumptions made, and (iv) show how the careful formalism of the general theory enables modular, self-consistent extensions that capture important features of the species and the problem in question. Perhaps the most difficult among the introduced concepts, the utilization (or mobilization) energy flow, is given particular attention in the form of an original and considerably simplified derivation. Specific examples illustrate a range of possible applications—from energy budgets of individual organisms, to population dynamics, to ecotoxicology.

Keywords: Dynamic Energy Budget, DEB theory, conservation laws, dissipation, reserve, structure

Contents

1. Introduction

The study of life and living organisms invariably crosses the borders of a single scientific discipline, inspiring interdisciplinary research and providing opportunities for important contributions from mathematics [1, 2], chemistry [3, 4], and physics [5, 6]. Dynamic Energy Budget (DEB) theory [7, 8] provides such an opportunity [9]. DEB is a formal metabolic theory of life [10] that represents an attempt to build a physics-like foundation for biological research [10, 11]. Its appeal originates from an unusual level of generalization and formalism attained through the guiding principle that the mechanisms responsible for running metabolism apply universally to the organisms of all species [8, 10, 11]. Identifying and formulating such universal mechanisms is largely in the domain of biology, but insights from other sciences, particularly thermodynamics [6, 12], have proven invaluable.

The interdisciplinary approach taken in the development of DEB theory, though successful, comes at a price—it introduces an abstract layer that forms a high barrier to entry [13]. In particular, the thermodynamic foundations of DEB theory remain disproportionately more accessible to physicists and mathematicians than biologists. Conversely, real-world applications in the form of individual-based bioenergetic models are mostly targeted at biologists, and as a consequence appear less palatable to physicists or mathematicians. Securing consistency across all disciplines, thus enabling each of the groups to focus on their interests without fear of incongruity between disciplines, is one of the chief strengths of DEB theory.

Having identified a dichotomy between the two aspects of the same theoretical body, we act to show in a manner accessible to a wide audience that the thermodynamic foundations and the resulting bioenergetic models integrate seamlessly with each other. We make a step forward from the existing literature by proving that the concept of energy (weak) homeostasis [14] can be mathematically formulated and derived from the common assumptions of DEB theory. To avoid being overly abstract and to supply readers with a practical guide to DEB-based modeling, we describe the standard DEB model in great detail, demonstrate its dynamics, and illustrate several applications. First, however, we turn to motivational considerations that list some reasons for the methodology adopted herein.

2. Occam's razor: The need for simplicity

The need for simplicity when mathematically describing living organisms has been acknowledged for at least 75 years [6]. Our aim is to take metabolism as a set of life-sustaining, enzyme-catalyzed chemical reactions occurring inside a living organism and capture the important aspects of the dynamics driven by these reactions in a systematic way. Because the number of possible reactions is vast, modeling all of them simultaneously would require an overwhelming level of detail and a vast number of potentially indeterminable parameters. We have little choice but to resort to (a high degree of) abstraction in an attempt to bring the complexity of the model down to a manageable level. Several properties of organisms encourage the pursuit of such an abstraction. We list some of these properties.

Limiting the amount of information. Out of approximately 90 naturally occurring elements, only 11 are ubiquitous in living organisms [15]. Out of these 11 elements, the main four (C, H, O,

and N) comprise about 99% of living biomass. A modeler, therefore, hardly needs to keep track of a large number of mass balances to capture the effects of many important metabolic processes. For example, mathematical expressions describing various components of the overall metabolism, such as growth or specific dynamic action, emerge from considerations that involve no more than the mass balances of the four main elements [13].

Focusing on aggregate (macrochemical) effects. In metabolic networks (i.e., graph-theoretical representations of metabolism), nodes corresponding to metabolites have an approximately scale-free degree distribution [16, 17]. The importance of this observation is twofold. First, metabolic networks are robust to random disruptions because most nodes (metabolites) are of small-degree and cannot cause a major loss of connectivity. Second, exceptionally high-degree nodes (hub metabolites) do exist and their presence is essential to the proper functioning of metabolic networks. In the modeling context, therefore, focusing on the aggregate (macrochemical) effects of hub metabolites may result in useful simplifications.

Cell similarity. The metabolic similarity of cells is mostly independent of organism size. The context here is much broader than the life cycle of a single individual. Once a successful metabolic pathway evolves, it can be preserved by evolution to serve very similar functions in various organs or even the same function in different species. A famous example is the cyclic AMP pathway used in cell communication by all animals investigated, including bacteria and other unicelluar organisms [18]. This pathway produces a cell-wide biochemical change that can last long after the outside stimuli stopped. Some responses triggered by the activated cyclic AMP pathway are (i) lipolysis in adipose tissue [18, 19], (ii) cardiac muscle contraction at an increased rate [18, 20], and (iii) the formation of short-term memory not only in humans, but also in such distant genera as *Aplysia* and *Drosophila* [21].

The simplifications and generalizations utilized by DEB may seem stretched, but are effective, and have been successfully applied for quite a while—even in clinical applications [6]. For example, the method of indirect calorimetry uses oxygen (O_2) consumption and carbon dioxide (CO_2) production to infer the net heat production of a whole organism [22]. The method thus makes a tremendous leap of distilling the complexities of such *in vivo* reactions as glucose, lipid, and protein oxidation, lipogenesis, and gluconeogenesis into the exchange of two gases with the environment. Nevertheless, the method is not only theoretically sound (see Section 5.3), but also used in numerous clinical contexts [23]. The need for simplicity, aside from these practical aspects, has epistemological and evolutionary origins that are discussed in the rest of this section.

2.1. The epistemological Occam's razor: The scientific reasons for simplicity

A simpler mathematical description of living organisms, i.e., the one with a lower number of variables and parameters, process-based and consistent with observed data, is better because its predictions are easier to test in practice [11]. Two aspects of this statement have been the subject of many discussions in the DEB-related literature.

The first aspect is the number of parameters and how they are estimated. If the axiomatic basis of a theory leads to models with many parameters that need to be estimated in applications, there is a danger of the curse of dimensionality—a situation in which the dimensionality of the model's

parameter space is so high that any practically attainable amount of data is sparse. In this situation, it becomes virtually impossible to obtain parameter estimates with reasonable statistical significance. The curse of dimensionality is a common theme in numerical analysis, combinatorics, machine learning, and data mining [24, 25, 26, 27, 28], but similar issues have been raised in relation to mechanistic models in climatology [29], ecology [30], and epidemiology [31, 32] to name a few examples. Given these circumstances, DEB theory has perhaps unsurprisingly been criticized for introducing too many parameters—nine in the standard DEB model to capture ontogeny (see Appendix A), and additional two to capture feeding on food of known density in the environment, and egg production. In a subsequent bid to make the standard model widely applicable, DEB theorists have devoted a lot of attention to parameter estimability [33, 34, 35, 36, 37, 38]; today, provisional parameter estimates can be calculated from existing sets using inter-species scaling arguments.

The second important aspect is the ability to generate testable predictions. Without doing so, theoretical work fails the criterion of falsifiability, and may be regarded as unscientific [39]. By generating predictions, however, we are able to refute any theory that is in irreparable disagreement with empirical data. The importance of this ability cannot be overstated as exemplified by the current state of affairs in the relationship between two physically sound metabolic theories in ecology: DEB, and Metabolic Theory of Ecology (MTE). MTE [40] has roots in nutrient supply network modeling [41] and aims to explain empirical observations that metabolic rates scale with species body size according to a 3/4 power law across some 20 orders of magnitude (see Section 7). The problem is that both DEB and MTE can serve as starting points to derive the same scaling equation, but do so for entirely different reasons [42]. Is it possible that both theories offer a valid basis for studying the fundamentals of biological form and function? This and similar questions have been at the heart of delicate discussions in the literature [43, 44], with the ultimate goal of finding empirical tests that may resolve the current conundrum [45, 46].

2.2. The evolutionary Occam's razor: evolutionary reasons for simplicity

Metabolic systems, ranging from a single pathway to the whole organism, are characterized by reaction rates and metabolite concentrations determined by a set of drivers such as enzymes, temperature, and externally available metabolites [47]. These drivers are subject to change due to environmental stimuli or stresses, followed by a regulated transition of the system to a new metabolic state. Without such a regulation, living organisms faced with the environmental variability would have to constantly adapt their physiology. Because the complexity of continuous physiological adaptations to a changing environment would be overwhelming, the evolutionary selection favored regulated internal conditions such that environmental changes are effectively filtered out and control of the metabolism is maintained. During evolution, therefore, organisms were able to develop several forms of maintaining the constant internal conditions commonly referred to as homeostasis [11].

2.3. Strong and weak homeostasis in DEB organisms

Metabolic systems are often found in a steady state with constant metabolite concentrations [6]. Even if the system is growing, the homeostatic regulation strives to maintain these concentrations

constant [47]. Consequently, the chemical composition of organisms should be remarkably stable. Does the evidence support such a conclusion?

Cyprinid fishes, for instance, exhibit only small differences in whole fish C, N, and P chemistry [48], and the variation of all chemical variables is lower in the fish than in the guts contents. These observations support the idea that the guts contents are driven by ingested material, whereas whole fish chemistry undergoes a homeostatic regulation observable even at the elemental level. Stoichiometric homeostasis is, in fact, so ubiquitous that it represents the key aspect for a branch of ecology called ecological stoichiometry [15]. This branch attributes much of the first-order commonality in the chemistry of living organisms to the homeostatic regulation. The same line of research also emphasizes second-order differences between species or functional groups. In general, autotrophs are more affected by the characteristics of their environment and exhibit less homeostatic regulation than heterotrophs [49]. The elemental content in heterotrophs largely reflects the differences in the allocation to major biochemical components.

To enable a simultaneous description of metabolism in mass, energy, and entropy terms, we need to assume that an organism is divided into conceptual compartments (generalized compounds) that have constant chemical composition and constant thermodynamic properties; this is referred to in DEB as strong homeostasis. Occam's razor urges us to minimize the number of generalized compounds that we consider while evidence supporting variability in stoichiometry suggests that one generalized compound is not enough. Typically, two generalized compounds are enough to describe stoichiometric variability in heterotrophs, while three or more are needed for autotrophs.

Empirical evidence suggests that the degree of homeostatic regulation in organismal stoichiometry is related to food conditions [50]. Under abundant food or constant food density, organisms are able to achieve a "perfect" homeostatic regulation, i.e., constant stoichiometry. This constancy is in DEB theory referred to as weak homeostasis. Because weak homeostasis is equivalent to a form of energy homeostasis (see Section 6.4), we use the terms energy and weak homeostasis interchangeably.

Thus, the organism's generalized compounds have constant chemical and thermodynamic properties regardless of (fluctuations in) available food. When the food is constant, the biomass as a whole also has constant chemical and thermodynamic properties.

2.4. Thermal homeostasis in DEB organisms

Endotherms are organisms that are able to maintain a constant body temperature (e.g., birds and mammals). The thermal homeostasis allows these species more independence from the environment because all metabolic rates depend on temperature [11]. This form of homeostasis comes with an additional energetic cost outside the thermoneutral zone (environmental conditions that do not require an increased metabolism to keep body temperature constant). Thermal homeostasis allows also for a higher body temperature, i.e., endotherms have higher internal body temperature when compared to ectotherms. Thus, endotherms eat, grow, and reproduce faster.

3. State variables

DEB theory is by no means limited to heterotrophic aerobes, yet we shall do so hereafter for clarity of exposition. The reason for imposing this limitation is that, as already mentioned, au-

totrophs exhibit less homeostatic regulation, thus generally requiring a more complex description in terms of three rather than two generalized compounds. Moreover, obligate aerobic metabolism characterizes almost all eukaryotic organisms, including plants, animals, and fungi.

3.1. State variables: material vs. non-material; requiring maintenance vs. not requiring maintenance

Biology provides a myriad of empirical evidence, often presented in a stylized form, that can serve as a foundation for theoretical developments [10, 11]. Among the empirical evidence that shapes the very core of DEB theory are observations made on organisms in the embryonic stage or during starvation. Embryos grow without food intake from outside sources, and most organisms survive short-term and sometimes even long-term starvation [51, 52, 53, 54, 55]. These facts suggest that the organic compounds necessary to run metabolic processes are provisioned for certain life stages or periods of suboptimal food availability. Hence, we assume that biomass in a heterotrophic organism is divided into two conceptual compartments (generalized compounds): reserve and structure. To distinguish reserve from structure in an intuitive manner, the former may be visualized as all tissue that does not require maintenance and is metabolizable as a source of energy. The latter consists of tissues that must be continuously maintained and are necessary for the survival of the organism.

Focusing on heterotrophic aerobes, DEB organisms are assumed to ingest food from the environment and egest feces back into the environment. Further interaction with the surroundings is assumed to occur through the exchange of four inorganic compounds: carbon dioxide (CO_2), water (H_2O), oxygen (O_2), and nitrogenous waste (predominantly ammonia (NH_3) in aquatic and uric acid ($C_5H_4N_4O_3$) or urea (CH_4N_2O) in terrestrial environments) [56]. Food is first assimilated (converted) into reserve. In the process, oxygen is taken from the environment while carbon dioxide, water, and ammonia are excreted as metabolites. Inefficiencies of the digestive system result in the egestion of organic matter in the form of feces. Growth is the conversion of reserve into structure in the presence of oxygen, with the already mentioned metabolites being released into the environment. Finally, energy from reserve is dissipated on processes that are necessary for the organism to stay alive and mature. The setting we just described—i.e., the basic assumptions on how heterotrophic aerobes function (Fig. 1)—reveal the natural candidates for capturing the state of a living organism. Therefore, we next briefly introduce the state variables of the DEB theory.

Material state variables. Based on the above considerations, four flows of organic compounds are readily identifiable. These flows are food ingestion, $\dot{J}_X$; assimilation into reserve, $\dot{J}_E$; growth, $\dot{J}_V$; and feces egestion, $\dot{J}_P$. Each flow quantifies the rate of change of one variable:

- Flow $\dot{J}_X$ governs the amount of ingested food (M_X), $\frac{dM_X}{dt} = \dot{J}_X$.
- Flow $\dot{J}_E$ governs the amount of amassed reserve (M_E), $\frac{dM_E}{dt} = \dot{J}_E$.
- Flow $\dot{J}_V$ governs the growth of structure (M_V), $\frac{dM_V}{dt} = \dot{J}_V$.
- Flow $\dot{J}_P$ governs the amount of egested feces (M_P), $\frac{dM_P}{dt} = \dot{J}_P$.

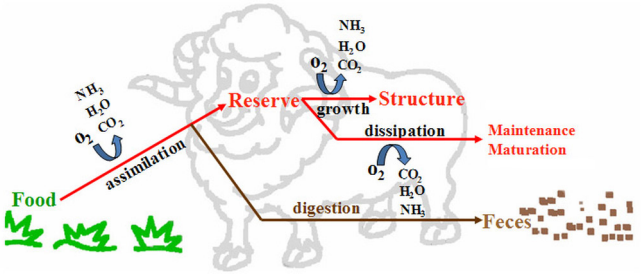

Figure 1: **Schematic representation of the basic metabolic processes in DEB organisms (heterotrophic aerobes).** Typically, food is assimilated into reserve in the presence of oxygen during which carbon dioxide, water, and nitrogenous waste are excreted into the environment. Reserve is used to power (i) growth, and (ii) various dissipative metabolic processes, where the latter keep the organism alive and allow it to mature. The egestion of feces occurs in parallel with assimilation due to the inefficiencies of digestive tracts.

Of the four listed variables, only two (M_E and M_V) represent the state of the organism. The other two are of interest when assessing the feed conversion ratios of the form $\frac{M_X}{M_E+M_V}$ or the digestibility coefficients of the form $1-\frac{M_P}{M_X}$. Such quantities are often used to measure performance in commercial activities such as aquaculture production [57, 58].

Non-material state variables. Along the life-cycle, organisms acquire new metabolic capabilities. For a typical multicellular organism, there is no feeding in the embryonic stage, the first feeding occurs at the onset of the juvenile stage, and reproductive events follow a transition to the adult stage. The material state-variables introduced so far are not able to fully describe the metabolism of organisms because stage transitions are only indirectly related to organismal growth; some species—the so-called indeterminate growers [59]—continue growing well into the adult stage, while others do not enter the adult stage well after growth has ceased. Furthermore, age and size at maturity depend on food availability [60, 61, 62]; and if food availability in the environment is poor, organisms may completely fail to enter the adult stage [63].

To account for these observations, additional state variable that quantifies the level of maturity (i.e., development) of the organism is needed. The level of maturity, M_H, increases with investment into maturation from zero at the initial embryo stage to M_H^b, the threshold that signals birth and triggers the feeding behavior, to M_H^p, the threshold that signals puberty and triggers allocation to reproduction. The maturity thresholds (M_H^b and M_H^p) are species-dependent parameters.

Notation. The chosen notation greatly facilitates understanding of DEB equations. Here, we lay out a set of notation rules that should, after an initial period of adaptation, be helpful in recognizing at a glance the type of quantity and its units.

Amounts: Capital M, E, and V denote the amount of a substance (units: C-mol for organic and mol for inorganic compounds), energy (unit: J), and volume (units: cm^3 or m^3), respectively.

Flows: All quantities represented symbolically by the capital J are the flows of substances (units: C-mol d^{-1} for organic and mol d^{-1} for inorganic compounds), while quantities symbolized by the small p are flows of energy (unit: J d^{-1}). A common phrase used to designate the flows of both substances and energy is metabolic flows or rates.

Dimensions: A dot on top of these symbols indicates the dimension of time^{-1}. Occasional appearance of curly braces indicates the dimension of area^{-1}. All symbols except V may appear in square braces indicating the dimension of volume^{-1}.

Indices for organic compounds: A set of indices for organic compounds is $\{X, V, E, P\}$, representing food, structure, reserve, and feces, respectively. In line with these definitions we can, for example, denote the amount of reserve by M_E, the energy fixed into structure as E_V, and the energy invested into maturity by E_H. Symbols E_E and V_V for energy contained in reserve and volume occupied by structure are usually written without indices.

Indices for inorganic compounds: An analogous set of indices for inorganic compounds is $\{C, H, O, N\}$, representing carbon dioxide, water, molecular oxygen, and nitrogenous waste, respectively.

Indices for basic powers: The three basic powers—assimilation, growth, and dissipation—are represented by the set of indices $\{A, G, D\}$. When considering flows of substances, indices for basic powers are sometimes combined with indices for organic or inorganic compounds to produce quantities such as $\dot{J}_{EA}$, indicating the flow of mass into reserve due to assimilation. In some equations, a star, $*$, is used as a wildcard index.

Yields: Lowercase letter y with two compound indices is reserved for yields when one compound is transformed into another. For example, y_{VE} denotes the yield of structure on reserve and arises from mass-balance considerations because these two compartments have a different chemical composition.

4. Transformations

Occam's razor and empirical evidence lead us to the definition of two material state variables in heterotrophic organisms: reserve and structure. The metabolic processes mentioned in the previous section (i.e., assimilation, growth, and dissipation) represent macrochemical transformations between the generalized compounds of reserve and structure. These transformations are summarized in Table 1.

Table 1: The three types of macrochemical reactions for a heterotrophic aerobe.

Assimilation	$y_{XE}\mathrm{CH}_{n_{HX}}\mathrm{O}_{n_{OX}}\mathrm{N}_{n_{NX}} + c_{11}\mathrm{O}_2 \rightarrow \mathrm{CH}_{n_{HE}}\mathrm{O}_{n_{OE}}\mathrm{N}_{n_{NE}} + c_{12}\mathrm{CO}_2 + c_{13}\mathrm{H}_2\mathrm{O} + c_{14}\mathrm{NH}_3 + y_{PE}\mathrm{CH}_{n_{HP}}\mathrm{O}_{n_{OP}}\mathrm{N}_{n_{NP}}$
Growth	$\mathrm{CH}_{n_{HE}}\mathrm{O}_{n_{OE}}\mathrm{N}_{n_{NE}} + c_{21}\mathrm{O}_2 \rightarrow y_{VE}\mathrm{CH}_{n_{HV}}\mathrm{O}_{n_{OV}}\mathrm{N}_{n_{NV}} + c_{22}\mathrm{CO}_2 + c_{23}\mathrm{H}_2\mathrm{O} + c_{24}\mathrm{NH}_3$
Dissipation	$\mathrm{CH}_{n_{HE}}\mathrm{O}_{n_{OE}}\mathrm{N}_{n_{NE}} + c_{31}\mathrm{O}_2 \rightarrow c_{32}\mathrm{CO}_2 + c_{33}\mathrm{H}_2\mathrm{O} + c_{34}\mathrm{NH}_3$
Symbols	$n_{*X}, n_{*V}, n_{*E}, n_{*P}$: chemical indices for food, structure, reserve, and feces y_{XE}, y_{PE}, y_{VE}: yields (food on reserve, feces on reserve, structure on reserve) c_{ij}, $i \in \{1, 2, 3\}$, $j \in \{1, 2, 3, 4\}$: stoichiometric coefficients

Section 2.3 introduces the concept of strong homeostasis. We are now in a position to provide a more technical definition of this concept and examine some basic implications thereof. Referring

to chemical indices in Table 1, the strong homeostasis assumption states that chemical indices and other thermodynamic properties for reserve and structure remain constant regardless of chemical indices for food. An immediate consequence is that acquiring an additional C-mole of, say, reserve always increases the internal energy of reserve by the same amount of joules. This amount is expressed in terms of molar enthalpy—a quantity representing the change in the internal energy of a system for every C-mole (mole) of an organic (inorganic) compound added to that system, i.e., $\bar{h}_* \equiv \partial U_*/\partial M_*$. Molar entropy, $\bar{s}_* \equiv \partial S_*/\partial M_*$, is another similarly defined quantity that remains constant under the strong homeostasis assumption. For the chemical (elemental) composition and the thermodynamic properties of the whole biomass to remain constant (weak homeostasis) even when the organism is growing (which occurs if the food conditions are stable), the ratio between the amount of reserve and structure must be fixed (see also Section 6.4).

4.1. The three fundamental transformations

What is the interpretation of the macrochemical reactions in Table 1? Taking assimilation as an example, we see that food gets transformed into reserve in the presence of oxygen, whereby building 1 C-mol of reserve requires ingesting y_{XE} C-moles of food and breathing in c_{11} moles of oxygen. In addition, y_{PE} C-moles of feces are produced because food cannot be processed fully in the digestive system. If we assume that reserve is assimilated at a rate $\dot{J}_{EA}$, these simple considerations imply a food ingestion rate of $\dot{J}_X = y_{XE}\dot{J}_{EA}$, and a feces egestion rate of $\dot{J}_P = y_{PE}\dot{J}_{EA}$. In addition, food assimilation accounts for a (variable) fraction of the organism's oxygen consumption by contributing amount $c_{11}\dot{J}_{EA}$ to the respiration rate ($\dot{J}_O$).

The process of assimilation also partly accounts for the excretion of carbon dioxide, water, and ammonia. While assimilated, food as a group of organic compounds with one aggregate chemical structure is being converted into reserve with another aggregate chemical structure. Due to the difference in the chemical structures of food and reserve, the conservation of mass implies a surplus in carbon, hydrogen, and/or nitrogen that must be excreted in some form. Heterotrophic aerobes typically excrete carbon dioxide, water, and ammonia. This excretion, much like oxygen consumption above, contributes $c_{12}\dot{J}_{EA}$, $c_{13}\dot{J}_{EA}$, and $c_{14}\dot{J}_{EA}$ to carbon dioxide ($\dot{J}_C$), water ($\dot{J}_H$), and ammonia ($\dot{J}_N$) flows, respectively, where coefficients c_{12}, c_{13}, and c_{14} are analogous to c_{11}.

Assimilated reserve is utilized for growth, or dissipated for maintenance and maturation. Growth involves the conversion of reserve into structure, meaning that 1 C-mol of reserve utilized for growth yields y_{VE} C-moles of structure. This conversion happens in the presence of c_{21} moles of oxygen, while c_{22}, c_{23}, and c_{24} moles of carbon dioxide, water, and ammonia, respectively, are being excreted for the same reasons as during food assimilation. Again, denoting the rate at which reserve is utilized for growth by $\dot{J}_{EG}$, we obtain that structure grows at a rate $\dot{J}_V = y_{VE}\dot{J}_{EG}$, while the corresponding contributions to flows $\dot{J}_O$, $\dot{J}_C$, $\dot{J}_H$, and $\dot{J}_N$ of inorganic substances are $c_{21}\dot{J}_{EG}$, $c_{22}\dot{J}_{EG}$, $c_{23}\dot{J}_{EG}$, and $c_{24}\dot{J}_{EG}$, respectively.

Reserve dissipated for maintenance and maturation—at a rate $\dot{J}_{ED}$—contributes only to the flows of inorganic substances. These contributions are $c_{31}\dot{J}_{ED}$, $c_{32}\dot{J}_{ED}$, $c_{33}\dot{J}_{ED}$, and $c_{34}\dot{J}_{ED}$ to $\dot{J}_O$, $\dot{J}_C$, $\dot{J}_H$, and $\dot{J}_N$, respectively. Lastly, the net reserve assimilation flow is $\dot{J}_E = \dot{J}_{EA} - \dot{J}_{EG} - \dot{J}_{ED}$. A summary of how all flows of organic and inorganic substances relate to the inflow into and outflows from reserve is given in Table 2, where the yields y_{XE}, y_{PE} and y_{VE} are species-dependent

parameters that account for the mismatch between the chemical compositions of food, reserve, and structure, as well as inefficiencies in conversion.

Any flow of substance that is consumed or produced by the organism is a weighted average of assimilation, dissipation, and growth rates (see Table 2). This means that metabolism has three degrees of freedom. If three flows are measured, e.g., oxygen consumption, and carbon dioxide and water production, then assimilation, dissipation, and growth can be estimated and used to compute any other flow.

Table 2: Flows of organic and inorganic compounds.

Flow of substance	Description
$\dot{J}_X = y_{XE}\dot{J}_{EA}$	Ingestion
$\dot{J}_V = y_{VE}\dot{J}_{EG}$	Growth
$\dot{J}_E = \dot{J}_{EA} - \dot{J}_{EG} - \dot{J}_{ED}$	Net reserve assimilation
$\dot{J}_P = y_{PE}\dot{J}_{EA}$	Egestion
$\dot{J}_O = c_{11}\dot{J}_{EA} + c_{21}\dot{J}_{EG} + c_{31}\dot{J}_{ED}$	Oxygen
$\dot{J}_C = c_{12}\dot{J}_{EA} + c_{22}\dot{J}_{EG} + c_{32}\dot{J}_{ED}$	Carbon dioxide
$\dot{J}_H = c_{13}\dot{J}_{EA} + c_{23}\dot{J}_{EG} + c_{33}\dot{J}_{ED}$	Water
$\dot{J}_N = c_{14}\dot{J}_{EA} + c_{24}\dot{J}_{EG} + c_{34}\dot{J}_{ED}$	Ammonia

4.2. Basal, standard, and field metabolic rates in DEB

In endotherms, basal metabolic rate (BMR) is defined as the metabolic rate of a fully grown fasting organism, at rest, in thermoneutral conditions [64]. In these conditions, assimilation and growth are null (i.e., $\dot{J}_{EA} = \dot{J}_{EG} = 0$) and dissipation is minimum because the organism is at rest and in thermoneutral conditions. For BMR measurements, only one flow, such as oxygen consumption, is enough to estimate dissipation and hence any other metabolic flow listed in Table 2.

BMR differs between endothermic species. One of the factors that contributes to these differences is body temperature, because BMR is measured in endotherms at their body temperature, which is species-specific. In contrast, ectotherms are organisms that have a variable body temperature and, consequently, have a variable basal metabolic rate. For these organisms, the BMR is measured at a reference temperature T_{ref}, and referred to as the standard metabolic rate (SMR). Some of the factors that explain these differences (such as the amount of structure) will be easier to understand in later sections, after more details on the physiological processes that comprise dissipation have been provided.

The application of Occam's razor suggests that organisms will have a higher and easier control over their own metabolism if all macrochemical transformations exhibit the same temperature dependence [7]. The temperature dependence of physiological rates is well described by the Arrhenius equation [65], which is consistent with empirical evidence that the logarithm of metabolic rates, such as reproduction or growth, decreases linearly with the inverse of absolute body temperature [7]. Arrhenius temperature, T_A, is the key parameter; the higher T_A (unit: K), the larger the

effects of temperature changes:

$$\ln \dot{J}_* (T) = \ln \dot{J}_* \left(T_{ref}\right) + \frac{T_A}{T_{ref}} - \frac{T_A}{T}, \tag{1}$$

where $\dot{J}_*$ is any of the flows summarized in Table 2. The Arrhenius description works well over a certain temperature range. At higher temperatures, the changes in metabolism-regulating enzymes could kill the organism; at lower ones, the metabolic rates are often below those predicted by the Arrhenius relationship. To compensate for these changes, an additional term, $\ln \gamma \left(T_{ref}\right) - \ln \gamma (T)$, can be added to Eq. (1), where function $\gamma = \gamma (T)$ is given by

$$\gamma (T) = 1 + \exp\left(\frac{T_{AL}}{T} - \frac{T_{AL}}{T_L}\right) + \exp\left(\frac{T_{AH}}{T_H} - \frac{T_{AH}}{T}\right). \tag{2}$$

Quantities T_{AL} and T_{AH} (unit: K) are constant parameters, and T_L and T_H (unit: K) are the lower and the upper boundaries of the organisms' temperature tolerance range [66]. Function $\gamma = \gamma (T)$ is always greater than unity, convex, and has a minimum between T_L and T_H. Because $\ln \gamma (T)$ in the extension of Eq. (1) comes with a minus sign, the role of $\gamma (T)$ is to decrease metabolic rates if temperatures are too high or too low.

When using the Arrhenius relationship, it is perhaps good to keep in mind that there is no mechanistic rationale for this relationship in the DEB theory. In fact, existing arguments [67] portray the Arrhenius relationship as a statistical formulation of an evolutionary outcome that at present cannot be derived from the first principles.

Superficially it may seem that the comparison of SMR for ectotherms is more straightforward than the comparison of BMR for endotherms because the rates are standardized to the same temperature. However, the chosen reference temperature changes the relative values of SMR among species because Arrhenius temperatures T_A are species-specific.

Finally, it is useful to make a clear distinction between basal and field metabolic rates (FMR). FMR is the average metabolic rate effectively expended by organisms over longer time periods going about their daily business of surviving [68]. In this case as opposed to BMR, assimilation and dissipation and possibly growth rates are positive, and a minimum of three flows are needed to estimate all other flows appearing in Table 2.

5. Thermodynamics

The first and second laws of thermodynamics apply to all living organisms. A living organism represents an open thermodynamic system that continuously exchanges compounds and heat with the environment, performs mechanical work, and disposes of internal entropy production. The first law was first tested in organisms by Max Rubner who in 1889 kept an adult dog in a calorimeter for 45 days measuring all input and output flows (food, feces, urine, and gases) and heat exchange. The measurement of heat exchange yielded 17,349 cal, while the difference between inputs and outputs yielded 17,406 cal. These values are almost identical [69] to the expected value if the dog's body mass changed only negligibly.

5.1. Types and relevance of heat, work, and mass flows

Analysis for a control volume [70] can help understand the implications of the laws of thermodynamics for DEB organisms. The control volume is an arbitrarily selected (often, but not necessarily fixed) volume of space through the boundary of which substances can pass in and out. In our case, the control volume is simply the organism itself, i.e., the volume of space bounded by the control surface at which all exchanges between the organism and the environment take place.

At the boundaries of the organism, flows include food, water, feces, nitrogenous waste, and gases such as oxygen and carbon dioxide among others. For the amount of substances, M, that comprise the biomass of the organism to be constant, the total input must equal the total output of substance, whereas the imbalance between these inputs and outputs determines the rate of change of M

$$\frac{dM}{dt} = \sum_i \left.\frac{dM_i}{dt}\right|_{in} - \sum_i \left.\frac{dM_i}{dt}\right|_{out}. \tag{3}$$

Here $i \in \{X, P\}$ for organic substances, and $i \in \{O, C, H, N\}$ for inorganic ones. Each amount of substance M_i can increase or decrease internal energy by $\bar{h}_i M_i$, where the molar enthalpy ($\bar{h}_i$) serves as a conversion coefficient. The internal energy is also affected by heat, Q, escaping or being received through the control boundary, as well as the mechanical work, W, performed by or on the organism. For internal energy U of the organism to be constant, the total energy input must equal the total energy output, whereas the imbalance between these inputs and outputs determines the rate of change of internal energy U:

$$\frac{dU}{dt} = \dot{Q} + \dot{W} + \sum_i \bar{h}_i \left.\frac{dM_i}{dt}\right|_{in} - \sum_i \bar{h}_i \left.\frac{dM_i}{dt}\right|_{out}. \tag{4}$$

To improve our intuition about the quantities appearing in this equation, it is useful to note [71] that within the animal kingdom (i) the heat transfer rate is relatively large and directed outwards ($\dot{Q} < 0$), (ii) the mechanical power is typically small and manifests itself as the work done on the surroundings ($\dot{W} \approx 0$, or possibly $\dot{W} < 0$), and (iii) the energy transfer associated with the inflows of compounds is typically much larger than associated with the outflows.

The mechanical power expenditure at the boundary is separable into expansion and non-expansion parts, i.e., $\dot{W} = p\frac{dV}{dt} + \dot{W}'$, where p is the pressure. At the surface of the Earth, the power expended on changes in volume is negligible, though this may not be the case in the deep ocean.

The non-expansion power expenditure $\dot{W}'$ is mostly associated with the movement of organisms, and therefore potentially relevant for very active species. Studies on the muscle efficiency suggest that the net muscle efficiency over a full contraction-relaxation cycle rarely exceeds 30% [72]. In a typical organism, therefore, over 70% of metabolic energy expended by the muscle is turned into heat rather than mechanical work.

Chemical reactions inside the organism release energy in the form of: (i) mechanical work such as external and internal muscle work, (ii) chemical work such as the maintenance of diffusion and chemical non-equilibrium, (iii) electrical work such as transmission of information, and (iv) heat. If the organism is in a steady state, i.e., mass and energy (and temperature) are constant, then all the internal work and internal heat release that result from metabolism end up escaping through

the boundary of the organism as "metabolic heat" via the heat transferring mechanisms such as radiation, convection, diffusion, and vaporization of liquid water. If "metabolic heat" is generated at a rate higher than the maximum possible rate for transfers through the boundary, the temperature of the organism increases. At a higher temperature, heat transfer mechanisms and all metabolic rates (see Eq. 1) pick up pace, and a new steady state is achieved.

Entropy in living organisms flows with substances, $\bar{s}_i M_i$, and with heat, $\frac{\dot{Q}}{T}$. For the internal entropy of the organism S to be constant, the total entropy input plus the entropy production must equal the total entropy output, whereas the imbalance between these inputs and production on one hand, and outputs on the other hand, determines the rate of change of entropy S,

$$\frac{dS}{dt} = \frac{\dot{Q}}{T} + \dot{\sigma} + \sum_i \bar{s}_i \left.\frac{dM_i}{dt}\right|_{in} - \sum_i \bar{s}_i \left.\frac{dM_i}{dt}\right|_{out} \tag{5}$$

A major difference between Eqs. (4) and (5) is that Eq. (5) has a an entropy production ($\dot{\sigma}$) term that serves as a measure of irreversibility, which cannot be measured at the boundaries of the organism.

5.2. Mass, energy, entropy, and exergy balances of DEB organisms

Mass balance. If the amount of substance, M, that comprises the biomass of an organism changes in time, this change must come either from depositing new or removing existing reserve or structure, i.e., $\frac{dM}{dt} = \dot{J}_V + \dot{J}_E$. Comparing with Eq. (3), we get

$$\dot{J}_V + \dot{J}_E = \dot{J}_X - \dot{J}_P + \dot{J}_O - \dot{J}_C - \dot{J}_N - \dot{J}_H. \tag{6}$$

Energy balance. Any change in the amounts of reserve and structure means that energy gets either deposited in or extracted from these compartments. Taking as a first approximation that the temperature of the organism is constant, the amounts of reserve and structure fully account for the changes in internal energy of the control volume, i.e., $\frac{dU}{dt} = \bar{h}_V \dot{J}_V + \bar{h}_E \dot{J}_E$. Comparing with Eq. (4), we readily obtain

$$\bar{h}_V \dot{J}_V + \bar{h}_E \dot{J}_E = \dot{Q} + \dot{W} + \bar{h}_X \dot{J}_X + \bar{h}_O \dot{J}_O - \bar{h}_P \dot{J}_P - \bar{h}_C \dot{J}_C - \bar{h}_H \dot{J}_H - \bar{h}_N \dot{J}_N \tag{7}$$

where $\bar{h}_i$, $i \in \{X, V, E, P\}$, represent the molar enthalpies of organic compounds (unit: J C-mol^{-1}). Similarly, $\bar{h}_i$, $i \in \{C, H, O, N\}$, stand for the molar enthalpies of inorganic compounds (unit: J mol^{-1}). The equation above represents the energy balance for DEB organisms in a non-steady state [12].

The energy balance may be applied to problems such as predicting spatial impact of climate change on biodiversity [73, 74]. Once the heat generation is quantified, it can be compared to the losses due to conduction, convection, and radiation. Ultimately, a body temperature implied by the given environmental conditions can be worked out. If, for example, the implied body temperature in the sun is outside the tolerance range of an organism, the organism may need to spend excessively long time in the shade, which could seriously hamper the organism's ability to catch prey and assimilate energy. The modeling approach allows testing of various climate change scenarios, and thus help determine critical environmental conditions in which the organism is no longer able to meet its maintenance requirements.

Entropy balance. Once again, any change in the amounts of reserve and structure means that entropy gets either deposited in or extracted from these compartments, i.e., $\frac{dS}{dt} = \bar{s}_V \dot{J}_V + \bar{s}_E \dot{J}_E$. Comparing with Eq. (5), we find that

$$\bar{s}_V \dot{J}_V + \bar{s}_E \dot{J}_E = \frac{\dot{Q}}{T} + \dot{\sigma} + \bar{s}_X \dot{J}_X + \bar{s}_O \dot{J}_O - \bar{s}_P \dot{J}_P - \bar{s}_C \dot{J}_C - \bar{s}_H \dot{J}_H - \bar{s}_N \dot{J}_N, \tag{8}$$

where $\bar{s}_i$, $i \in \{X, V, E, P\}$, denote the molar entropies of organic compounds (unit: J C-mol^{-1} K^{-1}), while $\bar{s}_i$, $i \in \{C, H, O, N\}$, denote the molar enthalpies of inorganic compounds (unit: J mol^{-1} K^{-1}). This equation represents the entropy balance for DEB organisms in a non-steady state [12] and provides a convenient way to quantify the entropy production.

By combining energy and entropy balances of living organisms in Eqs. (7) and (8), and taking into account that $\bar{\mu}_i = \bar{h}_i - T\bar{s}_i$, we obtain

$$\bar{\mu}_V \dot{J}_V + \bar{\mu}_E \dot{J}_E = T\dot{\sigma} + \dot{W} + \bar{\mu}_X \dot{J}_X + \bar{\mu}_O \dot{J}_O - \bar{\mu}_P \dot{J}_P - \bar{\mu}_C \dot{J}_C - \bar{\mu}_H \dot{J}_H - \bar{\mu}_N \dot{J}_N, \tag{9}$$

where $\bar{\mu}_*$, is the chemical potential (unit: J C-mol^{-1}). To better understand the meaning of $\bar{\mu}_*$ let us take a closer look at the left-hand-side of Eq. (9). Changes in internal energy and entropy are given by $\frac{dU}{dt} = \bar{h}_V \dot{J}_V + \bar{h}_E \dot{J}_E$ and $\frac{dS}{dt} = \bar{s}_V \dot{J}_V + \bar{s}_E \dot{J}_E$, respectively. A combination of the last two equations gives

$$\frac{dU}{dt} - T\frac{dS}{dt} = \left(\bar{h}_V - T\bar{s}_V\right)\dot{J}_V + \left(\bar{h}_E - T\bar{s}_E\right)\dot{J}_E. \tag{10}$$

Constant molar enthalpies and entropies, due to strong homeostasis assumption, allow us to perform the integration of both sides, resulting in

$$U - TS = \left(\bar{h}_V - T\bar{s}_V\right)M_V + \left(\bar{h}_E - T\bar{s}_E\right)M_E. \tag{11}$$

On the left, we recognize the definition of the total Gibbs free energy contained in the control volume, while right-hand side represents the sum of Gibbs free energies in reserve and structure compartments. The strong homeostasis assumption, therefore, implies that Gibbs free energy, G_*, is proportional to the amount of substance, M_*, where the proportionality constant is the chemical potential, $\bar{\mu}_*$.

Eq. (9) allows us to estimate the maximum theoretical amount of external work, i.e., work that an organism would perform if it could function without entropy production. For a steady-state organism, such that $\bar{\mu}_V \dot{J}_V + \bar{\mu}_E \dot{J}_E = 0$, this maximum work is called exergy and is equal to the net balance of Gibbs free energies. The exergy increases with the difference between the Gibbs free energy of the inputs (food and oxygen) and the Gibbs free energy of the outputs (feces, carbon dioxide, water, and nitrogenous waste).

5.3. Indirect calorimetry: the linear relation between flows

When mechanical power at the boundary of the control volume is negligible, e.g., when an organism is at rest, Eq. (7) can be used to quantify the organism's net heat generation. First, from the definitions in Table 2, we can express the reserve inflow and outflows in terms of oxygen, carbon dioxide, and nitrogen flows (basically by solving a system of three equations with three

unknowns). The resulting expressions can then be used to redefine all other flows of substances (see Section 4.1). Inserting these expressions into Eq. (7) would allow the inference of the organism's net heat generation solely from gas exchange measurements. Such a possibility is exploited in indirect calorimetry [22] and the subsequent array of modern-day clinical applications [23].

5.4. Relating heat and entropy production

Assimilation, dissipation, and growth are the three fundamental, macrochemical transformations taking place in conceptual biological reactors that are in a steady state. If we (i) make energy balances for these three biological reactors, (ii) assume that for most important biological aerobic reactions $T\Delta s$ is very small compared to Δh, and therefore Δh is approximately equal to $\Delta\mu$ [71], and (iii) sum the three energy balances, we obtain:

$$\bar{\mu}_V \dot{J}_V + \bar{\mu}_E \dot{J}_E = \dot{Q} + \dot{W} + \bar{\mu}_X \dot{J}_X + \bar{\mu}_O \dot{J}_O - \bar{\mu}_P \dot{J}_P - \bar{\mu}_C \dot{J}_C - \bar{\mu}_H \dot{J}_H - \bar{\mu}_N \dot{J}_N. \tag{12}$$

By combining the last equation with Eq. (9), we conclude that for aerobic organisms all entropy production is dissipated in the form of heat $T\dot{\sigma} = \dot{Q}$. The higher the temperature at the boundary of the control volume, the lower the entropy released per unit of heat dissipated. This means that the organism needs to dissipate more heat to get rid of the same amount of entropy. However, a higher temperature usually accompanies better regulated metabolism, which increases entropy production and implies an even higher need to dissipate heat. The result $T\dot{\sigma} = \dot{Q}$ means that for aerobic organisms the heat production is a good measurement of entropy production [12].

5.5. Measuring the entropy of living organisms vs. measuring the entropy of dead biomass

The result $T\dot{\sigma} = \dot{Q}$ implies that for aerobic organisms the entropy balance, Eq. (5), simplifies to

$$\bar{s}_V \dot{J}_V + \bar{s}_E \dot{J}_E = \bar{s}_X \dot{J}_X + \bar{s}_O \dot{J}_O - \bar{s}_P \dot{J}_P - \bar{s}_C \dot{J}_C - \bar{s}_H \dot{J}_H - \bar{s}_N \dot{J}_N, \tag{13}$$

which means that the specific entropies of reserve $\bar{s}_E$ and structure $\bar{s}_V$ can be estimated from entropy flows at the boundary of the control volume, and that the specific entropy of biomass ($\frac{s_V M_V + s_E M_E}{M_V + M_E}$) can be estimated as a function of reserve density [12]. Specific entropies for biomass obtained using this method for *Klebsiella aerogenes* are significantly different from the entropy of biomass given by Battley's empirical rule [75]. Because Battley's rule has been validated with good results for dead biomass and organic compounds [12], this difference suggests that the entropy of living biomass is different from the entropy of dead biomass.

By combining Eq. (13) with Eq. (6) and those found in Table 2, we have a system with 10 equations and 11 unknowns for aerobic organisms. If food conditions ($\dot{J}_X$) or any other flow are known then all other flows can be estimated. Aerobic metabolism has only one degree of freedom.

5.6. An energy description of dynamics in DEB organisms

In Section 5.2, we have seen that the strong homeostasis assumption implies proportionality between Gibbs free energy, G_*, and the amount of substance, M_*, with chemical potential, $\bar{\mu}_*$, as the constant of proportionality. However, the usual notation does not emphasize the fact that we are working with Gibbs free energy. Instead of symbol G_*, it is customary to use $E = \bar{\mu}_E M_E$ for the reserve compartment, and $E_i = \bar{\mu}_i M_i$, $i \in \{X, V, P\}$ for the other state variables.

Chemical potentials relate flows of substances to energy flows in the same manner in which they relate amounts of substances to Gibbs free energies. It is particularly useful to focus on the inflow into reserve, $\dot{J}_{EA}$, and outflows from reserve, $\dot{J}_{EG}$ and $\dot{J}_{ED}$, because (as emphasized in Table 2) all other flows of substances can be expressed in terms of these three. Here, indices A, G, and D, stand for assimilation, growth, and dissipation, respectively. We are now in a position to define assimilation, growth, and dissipation energy flows by $\dot{p}_i \equiv \bar{\mu}_E \dot{J}_{Ei}$, $i \in \{A, G, D\}$, thus making it possible to track the state of an organism in units of energy as summarized in Table 3.

Table 3: Dynamic equations in units of energy.

Equation	Description
$\frac{dE_X}{dt} = \kappa_A \dot{p}_A$	Ingestion
$\frac{dE}{dt} = \dot{p}_A - \dot{p}_G - \dot{p}_D$	Reserve dynamics
$\frac{dE_V}{dt} = \kappa_G \dot{p}_G$	Growth
$\frac{dE_P}{dt} = \kappa_P \dot{p}_A$	Egestion
$\kappa_A \equiv y_{XE} \frac{\bar{\mu}_X}{\bar{\mu}_E}$	Assimilation ratio[a]
$\kappa_G \equiv y_{VE} \frac{\bar{\mu}_V}{\bar{\mu}_E}$	Growth efficiency
$\kappa_P \equiv y_{PE} \frac{\bar{\mu}_P}{\bar{\mu}_E}$	Egestion efficiency

[a]In DEB-based literature (e.g., [7, 60]), it is customary to define the assimilation efficiency as $\kappa_X \equiv 1/\kappa_A$. For all efficiencies, it holds $0 < \kappa_* < 1$, whereas $\kappa_A > 1$.

6. From theory to applications: the standard DEB model

Discussion so far aimed at deducing the simplest, general equations possible for mass, energy, and entropy balances of living organisms. We achieved this aim by treating organisms as open thermodynamic systems in a non-steady state. Despite the deliberate search for simplicity, we ended up introducing a rather inconvenient layer of abstraction in the form of non-observable state variables that need to be related to measurable quantities.

6.1. Measurable quantities as functions of the abstract state variables

Biomass. Let us briefly consider the problem of linking relatively abstract state variables to frequently measured quantities such as biomass (units: g or kg) or the length of an organism (units: cm or m). To get an expression for biomass, we can combine the molar masses of structure and reserve, w_i, $i \in \{V, E\}$ (unit: $\mathrm{g\,C\text{-}mol^{-1}}$), with their respective chemical potentials, μ_i, $i \in \{V, E\}$ (unit: $\mathrm{J\,C\text{-}mol^{-1}}$), into ratios $w_i/\bar{\mu}_i$, $i \in \{V, E\}$ (unit: $\mathrm{g\,J^{-1}}$) that contain the information on how mass relates to energy. The molar mass values follow from chemical indices in Table 1, but it is important to keep in mind whether generalized compounds are given in hydrated form or not. Usually non-hydrated form is preferred, meaning that if d_E and d_V are the proportions of water in reserve and structure, respectively, (wet) biomass W is given by

$$W = \frac{w_E}{d_E \bar{\mu}_E} E + \frac{w_V}{d_V \bar{\mu}_V} E_V. \tag{14}$$

Two terminological and conceptual issues are worth emphasizing in the context of Eq. (14). First, the biological literature traditionally refers to biomass as the weight of organisms, although weight is technically a force and should be expressed in newtons rather than grams or kilograms. Symbol W is in fact the remnant of a such tradition. In a similar fashion, molar masses are often termed molecular weights. Second, the amounts of substances, M_*, are often called (molar) masses in DEB-based literature. This may not come as a surprise in view of the strong homeostasis assumption which guarantees proportionality between the amount of substance and the corresponding mass. Biomass, however, cannot be tracked in C-moles because chemical composition of the whole organism generally varies, even in DEB.

Structural volume and physical length. Before getting an expression for the measurable length of an organism, we consider the volume occupied by non-hydrated structure, V, also referred to as structural volume. Here, we rely on the observation that the wet density of organisms is generally close to $d_w \approx 1\,\mathrm{g\,cm^{-3}}$. To obtain the information on how dry structural mass relates to structural volume, we define a new quantity, the specific structural mass: $[M_V] \equiv d_w d_V/w_V = 1\,\mathrm{g\,cm^{-3}} \times d_V/w_W$ (unit: C-mol cm^{-3}). The volume occupied by structure is then $V = M_V/[M_V]$.

Another associated quantity is structural length, L, which can be defined as $L \equiv V^{1/3}$. Using these definitions and conversions $E_V = \bar{\mu}_V M_V$ and $M_V = [M_V]\,V$, it is possible to rewrite the growth equation in Table 3 in terms of structural volume or length. We obtain

$$\frac{dV}{dt} = \frac{\kappa_G}{\bar{\mu}_V\,[M_V]}\dot{p}_G = \frac{\dot{p}_G}{[E_G]}, \text{ and} \tag{15}$$

$$\frac{dL}{dt} = \frac{\dot{p}_G}{3L^2\,[E_G]}, \tag{16}$$

where $[E_G] \equiv \bar{\mu}_V\,[M_V]\,/\kappa_G$ is the volume-specific cost of structure (unit: J cm^{-3}).

Structural length, because it cannot be measured, is not yet a solution to our problem of linking the state variables to the measurable length of an organism. Bridging the gap between structural length and some measurable length of the organism is made possible by assuming isomorphism. The assumption is an approximation and rests on the observation that many organisms, at least in a given life stage, change their shape very little [76, 77, 78, 79, 80]. A striking example of isomorphism in action are the shapes of the organisms with a permanent exoskeleton [81]. The crucial aspect for us, however, is the fact that the ratio of two arbitrarily chosen lengths of an isomorphic organism is constant throughout the entire lifetime. Hence, any measurable length of the organism unaffected by the state of reserve, L_w, and structural length, L, are related by $L = \delta_M L_w$, where δ_M is a constant shape factor. A cubically shaped organism would have $\delta_M = 1$, if L_w were one of its sides, while a spherically shaped organism would have $\delta_M = \sqrt[3]{\pi/6}$, if L_w were its diameter. Many Osteichthyes (bony fish), for which a natural L_w is fork length, are characterized by $\delta_M \approx 0.2$ [7].

6.2. Relating metabolic processes to the state variables: scaling-based considerations

Assimilation. The discussion here focuses on the supplementary assumptions needed to specify how assimilation and dissipation energy flows depend on the state variables. We choose the assimilation of energy as a starting point. The main idea is that an organism needs some time, t_1,

to find and some time, t_2, to process food. For the processing time, we proceed from the fact that ingestion takes place over the control surface separating the organism from the environment. The larger the control surface, the more food is processed in any given time period. In the case of an isomorphic organism, the area of the control surface is proportional to the structural surface area, S, defined as $S \equiv L^2$. When the organism stops growing, the ability to process food becomes limited by the type and characteristics of the feeding apparatus. If $\left\{\dot{J}_{XAm}\right\}$ denotes the maximum surface-area-specific ingestion rate of a given feeding apparatus (unit: C-mol cm^{-2} d^{-1}), then we have $t_2^{-1} = \left\{\dot{J}_{XAm}\right\} L^2$, meaning that the food processing rate is assumed to scale with squared structural length. Note that t_2 is a time measure given in days per C-mole.

The next step is to find a similar expression for t_1. The time between two successive encounters with edible items must depend on the density of food in the environment X (unit: C-mol m^{-3}) because finding an edible item is easier when food density increases and vice versa. Considering as an example a motile organism that searches its surroundings with an average cruising speed $\dot{v}_{avg}$, the volume searched per unit of time can be expressed as $S_{eff}\dot{v}_{avg}$, where S_{eff} is surface area effectively accessible to the sensing organs. In the case of a growing isomorph, S_{eff} increases proportionally to the surface area of the sensing organs, which is in turn proportional to structural surface area. Consequently, $S_{eff}\dot{v}_{avg} = \left\{\dot{F}_m\right\} L^2$, where $\left\{\dot{F}_m\right\}$ is the surface-area-specific searching rate (unit: m^3 cm^{-2} d^{-1}; here the cubic meter pertains to the environment, while the square centimeter pertains to the organism). We can now write $t_1^{-1} = X\left\{\dot{F}_m\right\} L^2$, meaning that the food searching rate, similarly to the processing rate, is assumed to scale with squared structural length. The ingestion rate thus becomes $\dot{J}_X = (t_1 + t_2)^{-1}$, which combined with $\dot{p}_A = \bar{\mu}_E \dot{J}_{EA}$, $\dot{J}_X = y_{XE}\dot{J}_{EA}$ (Table 2), and a little algebra gives the expression for the assimilation energy flow

$$\dot{p}_A = \bar{\mu}_E \frac{\left\{\dot{J}_{XAm}\right\}}{y_{XE}} \frac{X}{\frac{\left\{\dot{J}_{XAm}\right\}}{\left\{\dot{F}_m\right\}} + X} L^2 = \{\dot{p}_{Am}\} f L^2. \tag{17}$$

In the above equation, the simplification on the rightmost hand side comes from the definition of the surface-area-specific maximum assimilation rate, $\{\dot{p}_{Am}\} \equiv \bar{\mu}_E \left\{\dot{J}_{XAm}\right\} / y_{XE}$ (unit: J cm^{-2} d^{-1}), and the Holling type II functional response, $f \equiv X/(K_X + X)$, where $K_X \equiv \left\{\dot{J}_{XAm}\right\} / \left\{\dot{F}_m\right\}$ is in ecology widely known as the half-saturation constant.

Somatic maintenance. Somatic maintenance, $\dot{p}_S$, is a part of maintenance costs associated with the existing structure. All eukaryotic cells continuously degrade and synthesize proteins in a series of biochemical processes collectively known as the protein turnover [82, 83, 84, 85, 86]. The energetic costs of the protein turnover [87, 88, 89, 90, 91] rise in proportion to the number of cells, which in turn is approximately proportional to structural volume. On the other hand, heating the body of an endothermic organism must counteract the heat loss through the outer surface. Therefore, the energy required to counteract the heat loss is proportional to structural surface. We can thus make a distinction between volume-related, $\dot{p}_M$, and surface-area-related, $\dot{p}_T$ somatic maintenance costs, where the following relationships are assumed to hold

$$\dot{p}_S = \dot{p}_M + \dot{p}_T = [\dot{p}_M] L^3 + \{\dot{p}_T\} L^2. \tag{18}$$

Proportionality constants $[\dot{p}_M]$ (unit: J cm^{-3} d^{-1}) and $\{\dot{p}_T\}$ (unit: J cm^{-2} d^{-1}) are called the volume-specific and the surface-area-specific somatic maintenance costs, respectively.

Maturation and maturity maintenance. In comparison to somatic maintenance, maturation and maturity maintenance are inferred from somewhat circumstantial empirical evidence, some of which was mentioned in Section 3.1. Furthermore, ubiquitous fitting of the von Bertalanffy growth model [92] to growth data for species that continue to grow in the adult stage would suggest that there is no growth retardation despite the sudden, considerable investment of energy into reproduction. If so is the case (but see [93, 94]), maturation is a metabolic process separate from growth, yet takes place and requires energy in parallel to growth.

The level of maturity, E_H, can be quantified by tracking the cumulative investment of energy into maturation. Quantity E_H is a non-material state variable whose rate of change is determined by maturation energy flow $\dot{p}_R$, i.e., $\frac{dE_H}{dt} = \dot{p}_R$. The stage transitions are assumed to occur when E_H crosses fixed threshold levels called maturity at birth, E_H^b, and maturity at puberty, E_H^p. Additionally, E_H^p is assumed to be the maximum level of maturity, because in the adult stage the maturation energy flow is redirected to reproductive activities (e.g., egg production).

One way to interpret the level of maturity is to identify it with the complexity of structure [10, 11], which in turn could relate maturation to the functioning of the genetic regulatory network. In line with the second law of thermodynamics, the complexity of structure would decrease without some form of maintenance. As a consequence, we assume that maturity maintenance energy flow $\dot{p}_J$ is proportional to the level of maturity, i.e., $\dot{p}_J = \dot{k}_J E_H$, where $\dot{k}_J$ is the maturity maintenance rate coefficient (unit: d^{-1}).

To better understand the concept of maturity maintenance, a comparison with volume-related somatic maintenance, $\dot{p}_M = [\dot{p}_M] L^3$, may be helpful. Upon recalling that energy in the structure compartment is $E_V = \bar{\mu}_V M_V$, and the amount of substance in this compartment relates to structural length via $M_V = [M_V] V$ and $V = L^3$, we obtain $\dot{p}_M = [\dot{p}_M] / (\bar{\mu}_V [M_V]) E_V$. The last relationship shows that $\dot{p}_M \propto E_V$, which is completely analogous to $\dot{p}_J \propto E_H$. However, there is an important difference between quantities E_V and E_H. The rate of change of the former is given by $\kappa_G \dot{p}_G$ (Table 3), but the rate of change of the latter is determined directly by $\dot{p}_R$. Growth efficiency, κ_G, reflects the dissipation of energy in the transformation of reserve into structure. By contrast, maturity is immaterial and therefore involves no such transformation. In applications, it is often convenient to work with a compound parameter, $\dot{k}_M \equiv [\dot{p}_M] \kappa_G / (\bar{\mu}_V [M_V]) = [\dot{p}_M] / [E_G]$, called the somatic maintenance rate coefficient (unit: d^{-1}). The roles of somatic and maturity maintenance rate coefficients are quite similar, but the analogy is incomplete as seen by contrasting $\dot{p}_M = \left(\dot{k}_M / \kappa_G\right) E_V$ with $\dot{p}_J = \dot{k}_J E_H$.

6.3. Relating metabolic processes to the state variables: the kappa rule

At this point, it is useful to take a closer look at energy flows out of reserve. There are two such flows; the growth flow, $\dot{p}_G$, and the dissipation flow, $\dot{p}_D$. Summing the two gives rise to the utilization (also mobilization or catabolic) flow, $\dot{p}_C = \dot{p}_G + \dot{p}_D = \dot{p}_G + \dot{p}_S + \dot{p}_R + \dot{p}_J$, which simplifies the reserve dynamics equation in Table 3 to

$$\frac{dE}{dt} = \dot{p}_A - \dot{p}_C. \tag{19}$$

Much like the other energy flows, the utilization flow is a function of the organism's state, i.e., $\dot{p}_C = \dot{p}_C(E, L)$. It is intuitive to ask what part of the utilization flow is used for somatic maintenance and growth as opposed to maturation in juveniles or reproduction in adults because, as mentioned before, these processes seem to take place in parallel. Therefore, without any loss of generality, we introduce a function $0 < \kappa(E, L) < 1$ to split the utilization flow into somatic and maturation (or reproduction) branches:

$$\kappa \dot{p}_C = \dot{p}_G + \dot{p}_S, \tag{20}$$

$$(1 - \kappa)\, \dot{p}_C = \dot{p}_R + \dot{p}_J. \tag{21}$$

Such a division would be rather impractical if κ were to depend on the state variables in a complex manner. The strong homeostasis assumption, fortunately, comes to the rescue with its two important consequences.

The first consequence of strong homeostasis is that the utilization flow is a homogeneous function of degree one with respect to energy in reserve. In mathematical terms, $\dot{p}_C(\lambda E, L) = \lambda \dot{p}_C(E, L)$, where $0 < \lambda < 1$ is a constant. To see why this result holds, let us for the moment entertain the notion that the reserve compartment, represented by an original generalized compound in total amount M, is decomposable into two more fundamental sub-compartments, represented by their own generalized compounds in amounts M_1 and M_2. Every C-mole of the original generalized compound mobilized from reserve will now be replaced with r C-moles of generalized compound 1 and $(1 - r)$ C-moles of generalized compound 2. We can say that $M_1 = rM$ and $M_2 = (1 - r)\, M$, where $0 < r < 1$. The strong homeostasis assumption then guarantees that r is a constant, because otherwise the ratio $M_1/M_2 = r/(1 - r)$ would be changing in time. This change would, in turn, imply a non-constant chemical composition of reserve, thus violating strong homeostasis.

Turning the amounts of substances into energies by means of chemical potentials, yields $E_1 = \lambda E$ and $E_2 = (1 - \lambda)\, E$, where $E_1 = \mu_E^1 M_1$, $E_2 = \mu_E^2 M_2$, $E = \mu_E M$, and $\lambda = r\mu_E^1/\mu_E$ is a constant. In addition, the ratio $E_1/E_2 = \lambda/(1 - \lambda)$ is also constant, meaning that for every joule of energy utilized from reserve exactly λ joules come from the first reserve sub-compartment (and $1 - \lambda$ joules from the second). Consequently, we have $\dot{p}_C(E_1, L)/\dot{p}_C(E, L) = \lambda$, which is equivalent to the first order homogeneity of function $\dot{p}_C = \dot{p}_C(E, L)$ with respect to variable E.

The second consequence of strong homeostasis—and the first order homogeneity of the utilization flow—is that κ is independent of energy in reserve. In mathematical terms, $\kappa(\lambda E, L) = \kappa(E, L)$. To obtain this result, we note that the somatic branch of the utilization flow, for the same reason as the total utilization flow above, is a first order homogeneous function with respect to variable E. This homogeneity implies that $\kappa(\lambda E, L)\, \dot{p}_C(\lambda E, L) = \lambda \kappa(E, L)\, \dot{p}_C(E, L)$. Applying $\dot{p}_C(\lambda E, L) = \lambda \dot{p}_C(E, L)$ onto the left side of the previous equality, we recover the expected result $\kappa(\lambda E, L) = \kappa(E, L)$, which proves that κ cannot be a function of energy in reserve. At best, $\kappa = \kappa(L)$. With the kappa rule in place, we can deduce several important results.

We start by showing that the organism grows to a finite size. From equations for reserve dynamics and growth in Table 3, we obtain that the total energy in reserve and structure satisfies $\frac{d}{dt}(E + E_V) = \dot{p}_A - \dot{p}_D - (1 - \kappa_G)\dot{p}_G = \dot{p}_A - \dot{p}_S - (1 - \kappa)\dot{p}_C - (1 - \kappa_G)\dot{p}_G$. Crucial in this equation is the interplay between $\dot{p}_A \propto L^2$ (Eq. 17) and $\dot{p}_S \propto L^3$ (Eq. 18), meaning that at some finite structural

size (L_∞), the somatic maintenance flow will be high enough to balance the equation's right-hand side. At this point, structure must stop growing because otherwise equality $\frac{dE}{dt} = -\frac{dE_V}{dt}$ implies $\dot{p}_A - \dot{p}_C = -\kappa_G \dot{p}_G \leq 0$, which leads to the depletion of reserve. The only sustainable situation for the organism is $\dot{p}_G = 0$ and thus $\dot{p}_A = \dot{p}_C$.

Inserting these sustainability conditions into the kappa rule gives an expression for the ultimate size, L_∞. Specifically, we have $\dot{p}_A = \dot{p}_S/\kappa$, from where the ultimate size is

$$L_\infty = \frac{\kappa\{\dot{p}_{Am}\}}{[\dot{p}_M]} f - \frac{\{\dot{p}_T\}}{[\dot{p}_M]}. \tag{22}$$

Here, it is natural to define two compound parameters. The first one is the maximum length, L_m, given by $L_m \equiv \kappa\{\dot{p}_{Am}\}/[\dot{p}_M]$ (unit: cm) beyond which the organism cannot grow even at the highest food level, $f = 1$. The second compound parameter is the heating length, L_T, given by $L_T = \{\dot{p}_T\}/[\dot{p}_M]$ (unit: cm), which determines how much surface-area related somatic maintenance costs reduce the ultimate size attainable by the organism irrespective of the food level.

Because the condition from which we obtain the ultimate size at constant f is $\dot{p}_A = \dot{p}_C$, energy in reserve also reaches its maximum value, E_∞, at this size. It is now of major convenience to define a state variable alternative to E—called the reserve density, $[E]$ (unit: J cm^{-3})—as the ratio of energy in reserve to structural volume, i.e., $[E] = E/V = E/L^3$. It immediately follows that the dynamics of the reserve density are given by

$$\frac{d[E]}{dt} = \frac{\dot{p}_A - \dot{p}_C}{L^3} - 3\frac{[E]}{L}\frac{dL}{dt}, \tag{23}$$

where the terms on the right-hand side arise directly from Eq. (19) and the chain rule $\frac{d[E]}{dt} = \frac{d}{dt}(E/L^3) = \frac{dE}{dt}/L^3 - 3E\frac{dL}{dt}/L^2$. The second term is often referred to as "dilution by growth" because it contributes to the decreases of the reserve density via the increase of structure. More importantly, the chain rule guarantees that pair $([E_\infty], L_\infty)$, where $[E_\infty] = E_\infty/L_\infty^3$, is a stationary point of Eq. (23) because both $\frac{dE}{dt}$ and $\frac{dL}{dt}$ are zero at E_∞ and L_∞, respectively. It is safe to say that this stationary point is a global attractor. Irrespective of the starting point, therefore, energy in reserve grows to E_∞ and structural length grows to L_∞, indicating that $[E] = E/L^3 \to E_\infty/L_\infty^3 = [E_\infty]$ as $t \to \infty$.

6.4. Relating metabolic processes to state variables: the energy mobilization theorem

Deriving dependence of the utilization flow on the organismal state variables is one of the more technical tasks in defining the standard DEB model. A simplified, pedagogical approach is pursued in Ref. [34], while Refs. [7, 10] provide the most details. Here we take a middle path to the main result by offering a standalone, rigorous, and novel—but still fairly understandable—treatment. Much of the preparatory work was, in fact, completed in the preceding section on the kappa rule.

To derive a mathematical expression for the utilization flow, we rely on a number of earlier results. Specifically, we use:

1. the reserve density equation, Eq. (23);
2. the stationary point of Eq. (23), i.e., $([E_\infty], L_\infty)$;

3. the assimilation flow, Eq. (17);
4. the somatic maintenance flow, Eq. (18);
5. the kappa rule, Eq. (20); and
6. the degree one homogeneity of the utilization flow with respect to reserve density, i.e., $\dot{p}_C(\lambda[E], L) = \lambda \dot{p}_C([E], L)$.

We append this list with one last assumption. The reserve compartment in DEB theory serves as a buffer that separates the relatively unstable environment from the relatively stable conditions maintained within an organism by homeostatic mechanisms [14, 95, 96, 97, 98]. To represent the effects of homeostatic mechanisms in our idealized framework, we assume that the metabolic processes powered from reserve are only implicitly dependent on food availability. In mathematical terms, $\frac{\partial \dot{p}_C}{\partial f} = 0$, which is the last ingredient needed to prove the functional dependence of the utilization flow on the state variables.

Theorem 1 (Energy mobilization). *If results 1.–6. hold and the utilization flow is only implicitly dependent on food availability ($\frac{\partial \dot{p}_C}{\partial f} = 0$), then energy is mobilized from reserve at a rate*

$$\dot{p}_C = \dot{p}_C([E], L) = [E] \frac{\dot{v}[E_G] L^2 + [\dot{p}_M] L^3 + \{\dot{p}_T\} L^2}{[E_G] + \kappa [E]}. \tag{24}$$

Proof. As a first step in proving the energy mobilization theorem, we rewrite Eq. (23):

$$\frac{d[E]}{dt} = \frac{1}{L^3}\left(\dot{p}_A - \dot{p}_C - \frac{[E]}{[E_G]}\dot{p}_G\right). \tag{25}$$

We then contrast this form with a general expression for the rate of change of $[E]$ ($\frac{d[E]}{dt}$), which follows from the result that $([E_\infty], L_\infty)$ is a stationary point of the reserve density, and from the Taylor's formula for a function of two variables:

$$\begin{aligned} \frac{d[E]}{dt} &= ([E] - [E_\infty])\dot{F}_1([E]) + (L - L_\infty)\dot{F}_3(L) \\ &+ (L - L_\infty)([E] - [E_\infty])\dot{F}_2([E], L), \end{aligned} \tag{26}$$

where $\dot{F}_i$, i =1, 2, 3 are unspecified functions. Derivatives in Eqs. (25) and (26) must be equal at all points, including $([E_\infty], L)$. We obtain

$$\frac{1}{L^3}\left(\dot{p}_A - \dot{p}_C - \frac{[E_\infty]}{[E_G]}\dot{p}_G\right) = (L - L_\infty)\dot{F}_3(L), \tag{27}$$

which, upon inserting Eq. (20) and some algebra, gives

$$\dot{p}_C([E_\infty], L) = \frac{[E_G]}{[E_G] + \kappa [E_\infty]}\left(\dot{p}_A + \frac{[E_\infty]}{[E_G]}\dot{p}_S + (L_\infty - L)L^3\dot{F}_3(L)\right). \tag{28}$$

The expression in Eq. (28) is beginning to resemble the desired result, but there are several problems. First, the appearance of the assimilation flow, $\dot{p}_A$, is problematic because this flow

explicitly depends on f—a direct violation of the assumption that $\frac{\partial \dot{p}_C}{\partial f} = 0$. We can find a way out, however, by noticing that $[E_\infty]$ and L_∞ originate from the same condition ($\dot{p}_A = \dot{p}_C$) and that $L_\infty = L_m f - L_T$ is explicitly dependent on f, indicating that the same must hold true for $[E_\infty]$. A function, $\dot{H} = \dot{H}([E_\infty])$, therefore exists such that $\dot{H}([E_\infty]) = \{\dot{p}_{Am}\}f$, where parameter $\{\dot{p}_{Am}\}$ is inserted out of convenience and without a loss of generality. Eventually, we generalize Eq. (28) out of the stationary state, thus replacing $[E_\infty]$ with $[E]$ and removing the explicit dependence on f. Another violation of assumption $\frac{\partial \dot{p}_C}{\partial f} = 0$ is due to the presence of the ultimate length, L_∞, in Eq. (28). In this case, however, a replacement analogous to the one just made is impossible because Eq. (28) is already out of the stationary state with respect to variable L. We therefore must conclude that $\dot{F}_3(L) = 0$. Summarizing these considerations yields

$$\dot{p}_C([E_\infty], L) = \frac{[E_\infty]}{[E_G] + \kappa [E_\infty]} \left(\dot{H}([E_\infty]) \frac{[E_G]}{[E_\infty]} L^2 + \dot{p}_S \right). \tag{29}$$

To finalize the proof, we generalize Eq. (29) out of stationary state $[E_\infty]$, while fully expanding the somatic maintenance flow in order to obtain

$$\begin{aligned} \dot{p}_C([E], L) &= \frac{[E]}{[E_G] + \kappa [E]} \left(\dot{H}([E]) \frac{[E_G]}{[E]} L^2 + [\dot{p}_M] L^3 + \{\dot{p}_T\} L^2 \right) \\ &+ ([E_\infty] - [E]) \dot{F}([E], L), \end{aligned} \tag{30}$$

where $\dot{F} = \dot{F}([E], L)$ is another, momentarily unspecified, function. Note that the presence of $[E_\infty]$ in the second term on the right-hand side of Eq. (30) would violate the assumption that $\frac{\partial \dot{p}_C}{\partial f} = 0$, unless $\dot{F}([E], L) = 0$.

The last remaining unknown in Eq. (30) is function $\dot{H} = \dot{H}([E])$. To determine this function, we rely on the result that the utilization flow is degree one homogeneous with respect to $[E]$. In this context, if reserve is subdivided into two or more sub-compartments, each of these sub-compartments is responsible for paying a fraction of somatic maintenance costs and for building a fraction of the structure, indicating that replacement $[E] \mapsto \lambda [E]$, $0 < \lambda < 1$ should be accompanied with replacements $[E_G] \mapsto \lambda [E_G]$, $[\dot{p}_M] \mapsto \lambda [\dot{p}_M]$, and $\{\dot{p}_T\} \mapsto \lambda \{\dot{p}_T\}$ (see also Section 2.3 in [7]). It turns out that the only form of function $\dot{H} = \dot{H}([E])$ compatible with degree one homogeneity of the utilization flow is linear, i.e., $\dot{H}([E]) = \dot{v}[E]$, where $\dot{v}$ is a new fundamental DEB parameter called the energy conductance (unit: $\mathrm{cm\,d^{-1}}$).

The energy mobilization theorem has multiple corollaries. In the following, we present in a formal manner perhaps the two most important ones.

Corollary 1 (Growth flow). *Given the conditions of Theorem 1, the growth flow is*

$$\dot{p}_G([E], L) = [E_G] \frac{\kappa \dot{v} [E] L^2 - [\dot{p}_M] L^3 - \{\dot{p}_T\} L^2}{[E_G] + \kappa [E]}. \tag{31}$$

Proof. Eq. (31) is obtained by inserting the utilization flow (Eq. 24) and the somatic maintenance flow (Eq. 18) into the kappa rule (Eq. 20), and solving for $\dot{p}_G$.

Corollary 2 (Energy or weak homeostasis). *Given the conditions of Theorem 1 and a constant food availability f, an organism with reserve density at birth $[E_b] = [E_\infty] = f\{\dot{p}_{Am}\}/\dot{v}$ will maintain this reserve density unchanged throughout the ontogeny.*

Proof. From Eq. (26), it s evident that $\frac{d[E]}{dt}\Big|_{([E_\infty],L)} \neq 0$ only if there is a term of the form $(L - L_\infty)\dot{F}_3(L)$. This term, however, turned out to be incompatible with assumption $\frac{\partial \dot{p}_C}{\partial f} = 0$, leading to the conclusion that $\dot{F}_3(L) = 0$. An expression for the utilization flow missing this term, such as the one given by Eq. (24), necessarily results in reserve density dynamics in which $\frac{d[E]}{dt}\Big|_{([E_\infty],L)} = 0$. At a constant reserve density the organism still grows as long as $L < L_\infty$ (verifiable from Eq. (31)).

With the above proofs completed, we are in a position to emphasize several interesting observations that pertain to energy (weak) homeostasis. In comparison with the many works so far, wherein the concept of energy homeostasis is presented as an assumption of DEB theory, here the same concept arises as a consequence of a more fundamental set of assumptions. Critical for the existence of energy homeostasis is the incompatibility of the term $(L - L_\infty)\dot{F}_3(L)$ in Eq. (28) with the assumption that $\frac{\partial \dot{p}_C}{\partial f} = 0$. By contrast, function $\dot{H} = \dot{H}([E])$ first appearing in Eq. (29) could have any form whatsoever, and energy homeostasis would still hold. The ultimate reason for the linearity of $\dot{H}([E])$ is traceable to strong homeostasis. Furthermore, we see that at maximum food availability ($f = 1$), the reserve density also reaches its maximum value $[E_m] = \{\dot{p}_{Am}\}/\dot{v}$. Finally, a constant reserve density translates into a constant ratio of the amounts of substances in reserve and structure, meaning that the chemical composition of organisms experiencing a constant food level is stable in time, which is the essence of weak homeostasis as stated initially (see Section 2.3).

6.5. The standard DEB model, simplifications, and dynamics

Gradually introducing the concepts of DEB theory in a logical sequence scattered the key equations, thus making it difficult to form a complete overview of the standard DEB model. To address this difficulty, energy flows are schematically presented in Fig. 2, while model equations and important symbols are summarized in Appendix A.

The closed form of the standard DEB model presented in Appendix A is general, but rather inconvenient for an intuitive grasp of the dynamics. Understanding the model dynamics is much easier by considering the scaled equations. To derive the scaled equations, we first need to scale the state variables. This scaling is quite natural given that we know the maximum reserve density, $[E_m]$, and maximum structural length, L_m, which allow us to introduce dimensionless quantities, $e \equiv [E]\,/\,[E_m]$ $(0 < e \leq 1)$ and $l \equiv L/L_m$ $(0 \leq l \leq 1)$ called the scaled reserve density and scaled structural length, respectively. It is convenient to supplement the new quantities with dimensionless scaled time, $\tau \equiv \dot{k}_M t$ as the independent variable, and dimensionless scaled heating length, $l_T \equiv L_T/L_m$ as a model parameter. Using these definitions in conjunction with the standard DEB model yields the scaled equations:

$$\frac{de}{d\tau} = g\frac{f - e}{l}, \tag{32}$$

$$\frac{dl}{d\tau} = \frac{g}{3}\frac{e - l - l_T}{e + g}, \tag{33}$$

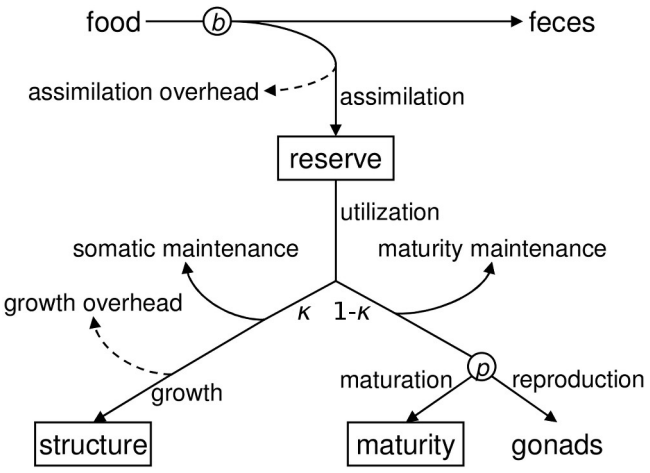

Figure 2: **Schematic representation of energy flows in the standard DEB model.** Commonly tracked state variables are denoted by rectangles. Nodes b and p indicate metabolic switches at birth (onset of feeding) and puberty (onset of reproduction). The utilization flow is split in accordance with the kappa rule. Overheads, quantitatively represented by assimilation and growth efficiencies, result from the chemical transformations of food into reserve and reserve into structure, respectively.

where $g \equiv [E_G] / (\kappa [E_m])$ is a compound parameter called the energy investment ratio. Multiple interesting conclusions on the dynamics of reserve and structure can be deduced from these equations.

The first conclusion on the basis of scaled equations is that the fate of reserve is determined by food availability in the environment. From Eq. (32), at $e = f$, the rate of change of the scaled reserve density equals zero, meaning that e is in a stationary state. This stationary state is a manifestation of energy (weak) homeostasis that we discussed previously. If, however, $e < f$, the rate of change of the scaled reserve density is always positive, meaning that e must increase towards f. This increase is faster when the difference between f and e is large, but gradually comes to a halt as e approaches f from below. Analogous reasoning applies to the opposite case, $e > f$, when e decreases and approaches f from above. Summarizing these conclusions in mathematical terms, at constant f, we have that $e \to f$ as $\tau \to \infty$. In addition, scaled size acts to slow down the reserve density dynamics, thus implying that larger individuals of the same species should be more resilient to the unfavorable feeding conditions and starvation. The trend that larger individuals better resist starvation is generally supported by observations [99, 100, 101, 102], but there are exceptions too [103].

The second conclusion based on the scaled equations is that the state of reserve determines the size of the organism. From Eq. (33), if $l + l_T = e$, the growth rate equals zero. If, however, $l + l_T < e$, the growth rate is positive, implying that $l + l_T$ increases towards e. The larger the difference between $l + l_T$ and e, the faster the growth. Conversely, as this difference gets smaller, the growth gradually ceases. In mathematical terms, we have that $l + l_T \to e$ as $\tau \to \infty$, which *is* the expected result, but we reached it without considering the possibility $l + l_T > e$.

Inequality $l + l_T > e$ corresponds to the state of food deprivation in which organisms are unable to cover somatic maintenance costs from reserve. To cover the immediate costs, as well as reduce

the need for somatic maintenance during prolonged food deprivation, organisms may shrink by metabolizing structure [7, 11, 104, 105]. However, there is an important difference between the growth and shrinkage: the former involves a conversion of reserve into structure accompanied by an overhead cost, whereas the latter does not. Because Eq. (33) incorporates such a growth overhead under all circumstances, using this equation during food deprivation would be incorrect.

Scaled equations tell us not only how the dynamics of reserve and structure unfold (i.e., $e \to f$ and $l + l_T \to e$ as $\tau \to \infty$), but also contain information on the relative time scales at which convergence takes place. Key quantity in this context is the energy investment ratio, g. As g becomes increasingly small, it takes more and more time for e to reach f, and for $l + l_T$ to reach e. Under such circumstances, both the dynamics of reserve and structure play an important role.

The situation changes as g increases. On the one hand, e becomes more and more responsive to f, up to the point where we can simply approximate the reserve density with food availability, i.e., $e \approx f$. On the other hand, when $g \gg e$, the energy investment ratio cancels out of the growth equation, leaving only structural length as the relevant state variable. An implication of these results is that for a range of moderate values of g, the reserve dynamics will be considerably faster than the growth. A reverse situation in which the growth is faster than the reserve dynamics cannot hold irrespective of the value of g.

Having a relatively fast-converging reserve dynamics would indicate that, at constant food availability, organisms would keep growing long after the scaled reserve density approached its stationary state. It is, therefore, meaningful to examine the growth of organisms when condition $e = f$ is satisfied. Under this condition, Eq. (33) is solvable and the solution is the well known von Bertalanffy growth curve [92, 106, 107, 108, 109].:

$$l = (f - l_T) - (f - l_T - l_b) \exp(-r_B \tau), \tag{34}$$

where $r_B \equiv \frac{1}{3} g/(f + g)$ is the dimensionless von Bertalanffy growth rate and l_b is the scaled length at birth (i.e., the initial condition). The curve in Eq. (34) is a monotonically increasing, concave function of time with one horizontal asymptote at $l_\infty = f - l_T$. When derived from the standard DEB model, von Bertalanffy curve for post-embryonic growth is determined by four compound parameters (L_m, g, $\dot{k}_M$, and l_T), but not all of them can be estimated from fitting this curve to data. Specifically, we would have to settle with estimates for $L_\infty = (f - l_T) L_m$ and $\dot{r}_B = \frac{1}{3} \dot{k}_M g/(f + g)$. If food availability was changing and reserve played a more prominent role, in addition to the four mentioned compound parameters, describing the post-embryonic growth would require a fifth parameter—the maximum reserve density, $[E_m]$.

For completeness, it is also necessary to define the scaled maturity density as a dimensionless quantity. One appropriate definition is $e_H \equiv E_H / \left(L^3 [E_m]\right)$. Consequently, the dynamics of the scaled maturity density are given by

$$\frac{de_H}{d\tau} = (1 - \kappa) \frac{ge}{l} \frac{l + g}{e + g} - e_H \left(k + \frac{g}{l} \frac{e - l}{e + g} \right), \tag{35}$$

where k is the dimensionless ratio of maturity to somatic maintenance rate coefficients, i.e., $k \equiv \dot{k}_J / \dot{k}_M$. Eqs. (32), (33), and (35) complete the mathematical formulation of ontogeny—from an egg to an adult individual—in accordance with DEB theory. It is now evident that in addition to

the five compound parameters already listed above, additional two parameters appear in Eq. (35); namely, κ and k. Two more parameters, scaled maturity densities at birth (e_H^b) and puberty (e_H^p), are needed to mark stage transitions, thus bringing the grand total to nine. What about the initial value of the scaled maturity density, e_H^0, at $\tau = 0$? An intuitive answer might be that an embryo at the beginning of its development should have zero scaled maturity density, but the mathematics is more tricky. In fact, a discussion on the initial conditions has purposely been avoided up to now due to considerable mathematical complexities [7, 110].

To say something about the initial conditions for the standard DEB model, we must start from the non-scaled state variables. At the beginning of embryonic development (i.e., at time $t = 0$), an egg is assumed to receive from its mother initial energy reserve E_0 [7, 110]. There is no structure, and the maturity level is zero. At $t = 0$, triplet (E, L, E_H) thus becomes $(E_0, 0, 0)$. We now encounter a difficulty because the value E_0 is unknown. There are also implications for the scaled state variables, some of which turn out to be ill-defined. The scaled reserve density, $e \equiv E/\left(L^3\,[E_m]\right)$, is initially infinite because it has a finite numerator (E_0), but zero denominator. Scaled structural length, $l \equiv L/L_m$, is simply zero, but the scaled maturity density, $e_H \equiv E_H/\left(L^3\,[E_m]\right)$, initially has zeros in both the numerator and the denominator, making it undetermined. However, using the fact that at scaled time $\tau = 0$, the condition $\frac{de_H}{d\tau} = 0$ is satisfied [7], Eq. (35) leads to the scaled initial maturity density given by $e_H^0 = (1-\kappa)\,g$. At $\tau = 0$, triplet (e, l, e_H) thus becomes $\left(+\infty, 0, e_H^0\right)$. Further details on the initial conditions, including an expression for the initial energy reserve, are presented in Appendix B.

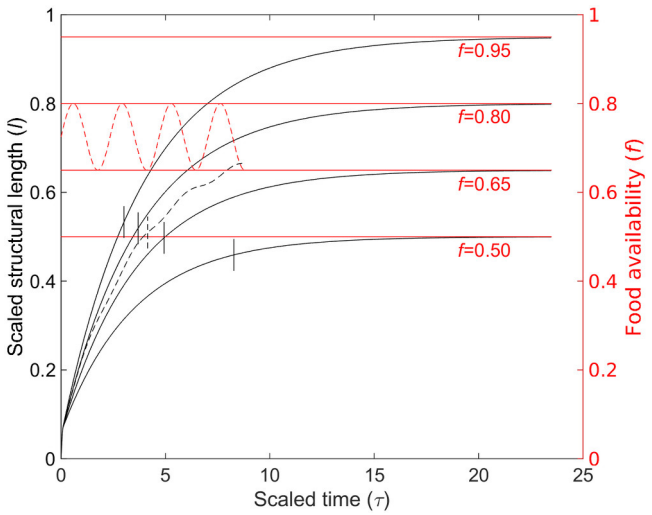

Figure 3: **Numerical illustration of the standard DEB dynamics.** Scaled structural length as a function of time is plotted at four constant and one sinusoidal food availability. The sinusoidal food availability oscillates between 0.65 and 0.80, with a scaled period of 2.35. Reserve dampens the effect of the variable environment, but at $\tau \approx 8.8$ the organism becomes large enough to experience food deprivation; when it does, Eq. (33) is no longer valid. Vertical bars indicate age- and length-at-puberty. Parameter values used in these simulations are: $[E_m] = 3375\,\mathrm{J\,cm^{-3}}$, $L_m = 3\,\mathrm{cm}$, $\dot{k}_M \approx 2.143 \cdot 10^{-3}\,\mathrm{d^{-1}}$, $g \approx 3.1111$ and $l_T = 0$.

The results of a numerical example are shown in Fig. 3. At four different, but constant, food availabilities, the solution to Eqs. (32) and (33) is the von Bertalanffy growth curve given by

Eq. (34). In this case, an organism's size increases monotonically towards the asymptote (i.e., the ultimate size) determined by the value of f. In a seasonal environment, in which f periodically oscillates, the growth curve also oscillates, but with a much lower amplitude. The reserve acts as a low pass filter between environmentally driven assimilation and relatively stable energy utilization. However, at scaled time $\tau \approx 8.8$ the organism becomes large enough to experience food deprivation (*sensu* $\kappa \dot{p}_C < \dot{p}_S$). The simulation was stopped at this point because, in line with the above explanation, applying Eq. (33) to shrinkage would violate energy conservation. Along with the size of the organism, we kept track of the scaled maturity density to illustrate how age and length at puberty change with food availability. As the value of f decreases, age at puberty increases because time required for the cumulative investment of energy into maturation to reach the level necessary for a stage transition increases as food decreases. Simultaneously, length at puberty decreases with f due to the considerable decline in the growth rate.

7. Allometry in DEB

Allometry describes by means of power laws the way biological traits such as oxygen consumption, life span, or reproduction rate change with the size of the organism. Allometry is a powerful tool because it reveals empirical patterns [69] that raise important research questions. For example, why does standard metabolic rate increase among living organisms with body mass raised to the power less than unity? This question, in fact, formulates the famous Kleiber's law [111] that originated from the work of Max Kleiber in the early 1930s and remained controversial to this day [112].

In the literature, allometric relationships typically fail to distinguish between intra- and inter-specific comparisons. However, the distinction between intra- and inter-specific scaling relationships is crucial because organisms are not only characterized by their size but also by their parameter values. In DEB theory, differently sized organisms of the same species share the same set of DEB parameters, yet differ in the values of state variables E, V, and E_H. Conversely, the organisms of different species have different parameter values.

Results provided by DEB intra- and inter-specific scaling relationships are indistinguishable from the empirical patterns revealed by allometry [7, 10]. However, DEB intra-specific relationships can be different from inter-specific relationships because each of these types of relationships arise from the different mechanistic explanations. A good example is provided by the explanations for Kleiber's intra- and inter-specific laws [11].

To obtain DEB inter-specific relationships we need to know how parameter values vary between species. The key aspect is to realize that some parameters, collectively called intensive, characterize processes that occur at a cellular level. The similarity between the cells of different species implies that intensive parameters (e.g., $\dot{v}$, κ, κ_R, $[\dot{p}_M]$, $\dot{k}_J$, and $[E_G]$) are roughly constant and are independent of the maximum size of the species. Other parameters (e.g., $\{\dot{p}_{Am}\}$, E_H^b, and E_H^p), called extensive, depend on maximum size in predictable ways; this dependence is mathematically expressed in the form of the functions of maximum size and intensive parameters [10]. An example is the maximum surface-area-specific assimilation rate, $\{\dot{p}_{Am}\} = L_m [\dot{p}_M] / \kappa$. In this expression, extensive parameter $\{\dot{p}_{Am}\}$ is proportional to maximum size (L_m), where the proportionality constant is the ratio of two intensive parameters, $[\dot{p}_M] / \kappa$.

We are now in a position to exemplify how intra- and inter-specific scaling of an energy flow may differ from one another. The focus is put on the assimilation flow ($\dot{p}_A$). From Eq. (17), we immediately obtain $\dot{p}_A \propto L^2$ intra-specifically. Inter-specific scaling, by contrast, is the functional dependence of biological traits on maximum size (L_m as opposed to L), meaning that in mathematical expressions (i) all appearances of L must be replaced with L_m and (ii) all extensive parameters must be expanded in terms of L_m. Applying (i) and (ii) onto Eq. (17) quickly yields $\dot{p}_A \propto L_m^3$ inter-specifically. Thus the assimilation flow increases with the squared structural length among the individuals of the same species, but the same flow increases with the cubed maximum structural length among the individuals of different species.

The maximum reserve density, $[E_m]$, is an ecologically important parameter because it indicates how well an organism withstands starvation. It is therefore useful to have at least an approximate idea if $[E_m]$ systematically varies with species size. From expression $[E_m] = \{\dot{p}_{Am}\}/\dot{v}$, it follows that $[E_m] \propto L_m$ because $\{\dot{p}_{Am}\} \propto L_m$ and $\dot{v}$ is an intensive parameter. Thus larger species should generally have a higher reserve density and hence better tolerate starvation than smaller species.

The fact that the parameters of the standard DEB model (see Appendix A for a summary) can be divided into intensive and extensive, naturally leads to the idea of parameter covariation [7, 11, 36, 37]. For all intensive parameters, on the one hand, we can expect that their values remain within a well-defined range irrespective of the species at hand. For example, if species 1 is characterized by energy conductance $\dot{v}_1$, while species 2 is characterized by $\dot{v}_2$, it should generally hold that $\dot{v}_1 \approx \dot{v}_2$. Although there are instances wherein intensive parameters differ considerably from one species to another (e.g., the volume-specific cost of structure, $[E_G]$, may easily vary by a factor of three depending on the water content of organisms), a reasonable bound on the values of these parameters suggests a certain reference—there should be some "default" (typical) values such that they represent a good starting point for parameter estimation whenever the standard DEB model is applicable.

For extensive parameters, on the other hand, we exploit their systematic dependence on the maximum species size to define the reference values at a predetermined maximum structural length, L_m^{ref}. If species 1 is the reference (i.e., $L_m^1 = L_m^{ref}$) with, say, maximum surface-area-specific assimilation rate $\{\dot{p}_{Am}^1\}$, then for species 2 we immediately have $\{\dot{p}_{Am}^2\} = \{\dot{p}_{Am}^1\} L_m^2/L_m^{ref}$, where L_m^2 is the maximum structural length of species 2. In general, ratio $z \equiv L_m/L_m^{ref}$ is called the zoom factor. Relationships such as $\{\dot{p}_{Am}\} = L_m [\dot{p}_M]/\kappa$ suggest that by setting $L_m^{ref} = 1\,\mathrm{cm}$ (or m), reference values for extensive parameters are determined entirely by the values of intensive parameters and hence approximately valid in any standard DEB model application. Because reference values should be a good place to start the estimation of model parameters or, alternatively, because similarly sized species should have similar parameter values, the method of parameter estimation employed in the DEB-based literature is often referred to as the covariation method [7, 11, 36, 37].

The discussion here is far from exhaustive, yet it illustrates the principles of obtaining ecologically relevant scaling relationships based on the standard DEB model. For a much more exhaustive treatment of the subject of allometry in DEB, the reader is referred to Refs. [7, 8, 10, 11, 36, 37].

8. DEB applications

The rigorous theoretical background and strict adherence to the laws of conservation of mass and energy allows for coherent applications and extensions of DEB models. As of the first quarter of 2016, there are more than 500 peer-reviewed papers on DEB and its applications (see [113] for a complete list), and DEB parameters for more than 400 species have been determined (see [114] for a complete list of species and parameter values). Clearly, any review of DEB applications shorter than a book can be cursory at best. We hope, however, that even a cursory review can give a useful overview of the type of problems DEB can be used for. To maximize the effect, our examples span applications ranging across scales of biological organization, types of organisms, and research questions. Inevitably, the choice of examples has been biased by interests, comprehension, and expertise of the authors. Hence, this section is not exhaustive; there are numerous additional existing and potential applications. We sincerely hope that the reader will find or devise one suitable for their research question(s).

We start by giving a short overview of the huge and growing database of standard DEB model parameters, and on a recent example (the loggerhead turtle) showcase the type of insights one might expect by applying a DEB model to a species. Next, we show examples of DEB model extensions that track metabolic products, predict distribution of toxicants, and enable coherent mechanistic approach to ecotoxicology. Finally, we discuss mortality, and show how DEB has been used to extrapolate environmental conditions to population-level dynamics, including population-level effects of toxicants.

8.1. Overview of the Add_my_pet collection—the on-line DEB model parameters database

The Add_my_pet collection currently houses 416 species belonging to 17 phyla [114], which is a 7-fold increase from 60 species present in the collection only 5 years ago [37]. Estimation of parameter values for new species has been simplified and can be done using four user defined scripts (`run`, `mydata`, `pars_init`, and `predict`) implemented in the software package DEBtool [115]. Over 70% of species for which the DEB parameters have been estimated belong to the Chordata phylum, with only two other phyla having more than 10 species represented: Mollusca (34 species, 8.2%) and Athropoda (50 species, 12%). A somewhat anthropocentric interest to study creatures that are our food (such as mollusks and crabs), or that eat our food (for example, insects) becomes even more obvious when we take a closer look at the Chordata phylum: over $> 30\%$ of studied species belong to Actinopterygii (for example, fish), and another $> 30\%$ of species are those closest to us—mammals. The third largest group are birds with 49 species represented, the majority of which are a result of recently performed work [116].

Such a vast and versatile collection reveals its huge potential when the parameter values are analyzed simultaneously for the patterns to emerge. Patterns in parameter values (e.g., sub optimal investment into reproduction mentioned in Ref. [37]) often are a part of a more general trend confirmed when the analysis is repeated using a larger sample size with more species [117] or studying several classes of a single group (e.g., fish [118]). Meta-analyses of parameter values have helped explain (i) metabolic acceleration in juveniles [119, 120], (ii) the wasteful use of resources to maximize growth during periods of plentiful resources [121], (iii) the position of animals on the

abstract supply-demand spectrum, including the resilience of organisms during periods of starvation [122], and (iv) the link between sensitivity to chemical compounds and animal metabolic rates [123].

While the collection of parameter values provides insights into potentially important evolutionary patterns, focusing on a single species (i.e., the corresponding parameters, model predictions, and the subsequent implications) offers insights into physiology and ecology of this species with important applications for resource management. Such management becomes especially relevant when the species of interest is commercially valuable and a major food source (e.g., fish [124]), or is an endangered species facing various threats despite the conservation measures, as is the case with six out of seven sea turtle species [125]. We showcase insights that can be gained from application of a DEB model to a species on the example of one of the largest nesting aggregations of the loggerhead turtle, the North Atlantic population [126].

8.2. Application of the standard DEB model—the case of the loggerhead turtle

Interest in studying the loggerhead turtles spans more than seven decades. For instance, the information on growth in captivity was published as early as in the 1920s [127, 128, 129]. Moreover, the need for an energy budget approach was identified almost a decade ago [130]. Despite this interest, data detailing energy utilization are scarce, a comprehensive life cycle analysis is hindered by disjointed data sets, empirical studies by necessity rarely share focus, and methodologies widely differ. The mechanistic nature of DEB models enables the assimilation of a wide variety of disjointed data sets, thus enabling much of the existing (published and unpublished) data to be used simultaneously.

To satisfy the need for an energy budget approach in loggerhead turtle research, we devised a full life cycle model based on DEB theory [131]. Data sets and sources used during the model development are listed in Table 4. Achieved data completeness level is estimated at between 3.5 and 4 on a theoretical scale of 1 to 10 defined in Ref. [36]. The parameter values of the standard DEB model (see Appendix A) were estimated using the covariation method (see Section 7; [36, 37]), although some values were used as found in the literature. All values are listed in Table 5.

The model yielded a very good description of the loggerhead turtle's life cycle [131], with a mean relative error (MRE) of 0.178. Generally, the MRE is negatively correlated with the data completeness level [37] because fitting a greater variety of data with the same number of parameters is bound to produce a comparatively worse albeit a more meaningful fit. The data completeness level of 3.5 for the loggerhead turtle is relatively high because all entries in the Add_my_pet collection have a completeness level below 5, and only approximately 3% of the species have the data completeness level above 3.5 [114]. The MRE of the loggerhead DEB model (0.178) is slightly above the average MRE of the Add_my_pet library (0.158), but lower than the MREs of 57.4% of library entries. Given the high data completeness level, this is an exceptional fit. Favorable goodness of fit was especially encouraging because certain information required to complete the whole life cycle had been incorporated in the model through simplifications, adjustments, and/or additional assumptions. For example, environmental conditions were assumed constant, with estimated average food availability of $f = 0.81$ and temperature of 21° C [149], even though loggerhead sea turtles are known to switch between distinctly different habitats during their life cycle [150].

Table 4: Types of data and data sources used for the parameter estimation: life-history traits (from A to K) and functional relationships (from a to h). SCL stands for straight carapace length.

	Life-history traits	Data source
(A)	age at birth[a]	[132, 133]
(B)	age at puberty	[134, 135, 136]
(C)	life span	[137, 138]
(D)	SCL at birth	[128, 129, 135]
(E)	SCL at puberty	[139, 140, 141, 142, 143]
(F)	ultimate SCL	[139, 140, 141, 142, 143]
(G)	wet body mass at birth	[132, 144]
(H)	wet body mass at puberty	[141, 142]
(I)	ultimate wet body mass	[140, 142]
(J)	initial energy content of the egg	[145]
(K)	maximum reproduction rate[b]	[146, 147]
	Functional relationships	Data source
(a)	Incubation duration vs. incubation temperature	[132]
(b)	Carapace length vs. age (captive post-hatchlings up to 10 weeks old)	[132], L. Stokes[c]
(c)	Body mass vs. age (captive post-hatchlings up to 10 weeks old)	[132], L. Stokes
(d)	Body mass vs. length (captive post-hatchlings up to 10 weeks old)	L. Stokes
(e)	Carapace length vs. age (captive juveniles and adults)	[127, 128]
(f)	Body mass vs. age (captive juveniles and adults)	[127, 128, 129]
(g)	Body mass vs. length (wild juveniles and adults)	[148]
(h)	Number of eggs per clutch vs. length (wild adults)	[143]

[a]Birth in DEB is defined as the moment when hatchlings start feeding, so age at birth was calculated by adding the average time between hatching (exiting the egg shell) and onset of feeding to the observed age at hatching.

[b]Maximum reproduction rate was expressed as eggs per day using the number of eggs per clutch (assumed to be 140 on average), the number of clutches per nesting season, and the number of nesting seasons per year (an inverse of the remigration interval). The maximum reproduction rate was then calculated as $R_i = 4 \times 140/(2.5 \times 365) = 0.7671$.

[c] Unpublished data courtesy of L. Stokes, Southeast Fisheries Science Center, National Marine Fisheries Service, Miami, Florida, United States of America.

Table 5: List of standard DEB model parameters for the North Atlantic loggerhead turtle (*Caretta caretta*). An additional shape parameter δ_{CL} was used for the data where the type of length measurement had not been specified [127, 128]. Preliminary parameter values for two other sea turtles in the Add_my_pet library are given for comparison: Kemp's ridley (*Lepidochelys kempii*) [151], and leatherback turtle (*Dermochelys coriacea*) [152]. Typical parameter values used to initiate the covariation estimation method are found in Refs. [7], Table 8.1, p. 300 and [36]. All rates are given at reference temperature $T_{ref} = 273\,\mathrm{K}$, and scaled food availability $f = 0.81$. Parameters for which the typical values were used as-is are listed below the table.

Parameter	Symbol	*C. caretta*	*L. kempii*	*D. coriacea*	Unit
Max. area-specific assimilation rate	$\{\dot{p}_{Am}\}$	906.1[a]	728.4	1191	$\mathrm{J\,d^{-1}\,cm^{-2}}$
Energy conductance	$\dot{v}$	0.07084	0.0424	0.0865	$\mathrm{cm\,d^{-1}}$
Allocation fraction to soma	κ	0.6481	0.6929	0.9166	-
Volume-specific somatic maint. rate	$[\dot{p}_M]$	13.25	20.1739	21.178	$\mathrm{J\,d^{-1}\,cm^{-3}}$
Volume-specific cost of structure	$[E_G]$	7847	7840.77	7843.18	$\mathrm{J\,cm^{-3}}$
Maturity at birth	E_H^b	3.809e+04	1.324e+04	7.550e+03	J
Maturity at puberty	E_H^p	8.730e+07	3.648e+07	8.251e+07	J
Arrhenius temperature	T_A	7000[b]	8000	8000	K
Shape coefficient	δ_M	0.3744	0.3629	0.3397	-
Shape coefficient	δ_{CL}	0.3085			-
Density of structure and reserve	d_V, d_E	0.28[c]	0.3	0.3	-

[a]Indirectly estimated parameter, $\{\dot{p}_{Am}\} = L_m^{ref} z\,[\dot{p}_M]/\kappa$, using the estimate of $z = 44.3$ for loggerhead turtles. *L. kempii*: $z = 25.0$, *D. coriacea*: $z = 51.6$.

[b] Estimated independently by direct fitting to the data on incubation duration vs. incubation temperature published in Refs. [132], [153], and [154].

[c] Value from Ref. [155].

Other parameters with typical values: Ingestion efficiency $\kappa_X = 0.8$; Reproduction efficiency, $\kappa_R = 0.95$; Maturity maintenance rate coefficient, $\dot{k}_J = 0.002\,\mathrm{d^{-1}}$; Egestion efficiency, $\kappa_P = 0.1$; Maximum searching rate, $\left\{\dot{F}_m\right\} = 6.51\,\mathrm{d^{-1}\,cm^{-2}}$.

Instead of discussing the model's goodness of fit in great detail, we showcase the type of information obtainable by applying the DEB model. For example, calculating the cumulative energy investment during embryonic period offers insights into the energy reserve available to post-hatchlings when they reach the offshore feeding grounds (Fig. 4).

The amount of assimilated energy and subsequent allocation thereof change as a loggerhead turtle grows and matures. Calculating and visualizing the allocation of mobilized energy between the processes of (somatic and maturity) maintenance, growth, and maturation (i.e., reproduction after reaching adulthood), allows us to better understand metabolism that shapes an individual's life cycle (Fig. 5). For example, the (rarely discussed) maturity maintenance comprises almost 25% of the energy budget of a fully grown adult (Fig. 5). Furthermore, while a juvenile individual retains anywhere between 40% (when younger) and 10% (when older) of the assimilated energy as reserve, once this same individual reaches its ultimate adult size, the mobilization flow, $\dot{p}_A$, equals the assimilation flow, $\dot{p}_C$ (Fig. 5). This equality implies a constant amount of reserve

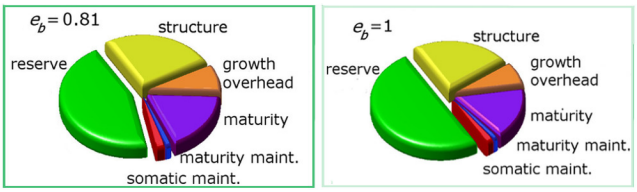

Figure 4: **Cumulative energy investment until birth (i.e., the moment of first feeding), including the remaining reserve.** Shown are the plots for two scaled functional responses, $f = e_b = 0.81$ and $f = e_b = 1$. At $f = 0.81$ (left panel), representative of the North Atlantic loggerhead turtle population, slightly less than half of the initial reserve is left at birth. The rest is dissipated into the environment or consumed for the growth of structure before birth. The exact fraction is important for further development and survival because the size of the remaining reserve (partly visible as the external yolk sac) determines, e.g., the period that hatchlings survive before reaching the feeding grounds. The DEB model also allows examining alternative scenarios. Shown is the case of maximum functional response $f = 1$ (right panel). A comparison between the two scenarios suggests a limited sensitivity to f experienced by the mother because the remaining reserve at birth changes only a little.

(Eq. 19). Because neither reserve nor structure change anymore, the reserve density (Eq. 23) is also maximal.

The maximum reserve density is an ecologically interesting parameter because it determines how well an individual withstands starvation. This parameter depends on the ratio of two other parameters: $\{\dot{p}_{Am}\}$ (determining reserve assimilation) and $\dot{v}$ (determining reserve mobilization). For a general discussion, however, a more intuitive quantity than the maximum reserve density is the time to reserve depletion, $t_\dagger$. Starving organisms after a while reach a point at which $\kappa \dot{p}_C = \dot{p}_M$ (i.e., when reserve energy is $E_* = \dot{p}_M \frac{L}{\kappa \dot{v}}$), meaning that the mobilization flow is about to become too low to satisfy the somatic maintenance needs under the kappa rule. Although there is no single general recipe for how organisms handle starvation within DEB theory [7], one reasonable alternative is to assume that enough energy is mobilized from reserve to maintain the existing structure. In this case, the time it takes for energy in reserve to drop from level $E = E_*$ to $E = 0$ is given by a particularly simple expression, $t_\dagger = \frac{L}{\kappa \dot{v}} = \frac{[E_m]}{[\dot{p}_M]} l$, where $l = L/L_m$ is the scaled structural length (see Section 6.5). If maturity is maintained as well, the time to reserve depletion shortens by factor $0 < \frac{\dot{p}_M}{\dot{p}_M + \dot{p}_J} < 1$. The larger the maximum reserve density, the longer the time to reserve depletion. The somatic maintenance cost, represented here by $[\dot{p}_M]$, has exactly the opposite effect. Finally, adults (larger l) better handle starvation.

The relatively low value of $[\dot{p}_M]$ (Table 5) and the relatively high value of $[E_m] = 12791\ \mathrm{J\,cm^{-3}}$ for the loggerhead turtle, indicate that an average adult of this species may spend up to a year in starvation before depleting reserve [131]. This result is in sharp contrast with the results for pelagic fish such as anchovies [156] and bluefin tunas [60, 124, 157]. For these species the ratio of $\{\dot{p}_{Am}\}$ and $\dot{v}$ keeps the maximum reserve density disproportionately small. Prime examples in this context are bluefin tunas, who are notable for their small reserve density compared to body size, the result of which is a life style typical of demand systems [122] summarized succinctly in the phrase “energy speculators”.

We conclude that the standard DEB model aided the characterization of the whole life cycle of the loggerhead turtle using only a relatively few disjointed data sets on life-history traits and

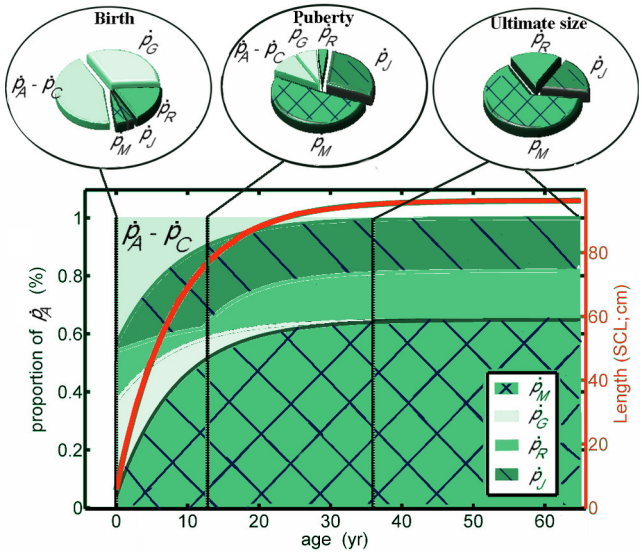

Figure 5: **Visualization of the full life cycle energy budget of the loggerhead turtle.** Insets zoom into energetically important moments—birth, puberty, and ultimate size. Shown are growth ($\dot{p}_G$), maturation/reproduction ($\dot{p}_R$), and somatic and maturity maintenance ($\dot{p}_M$ and $\dot{p}_J$, respectively) energy flows as the fractions of the daily energy intake. Parameter values correspond to North Atlantic population (Table 5) experiencing the scaled food availability of $f = 0.81$.

growth, some of which date from 1926. This and similar models thus offer an opportunity to bridge the knowledge gaps and help understand the life cycle of endangered species. The model can further be used to study the environmental effects on metabolic processes such as growth, maturation, and reproduction, as well as explore future scenarios, e.g., those resulting from the global climate change. Ultimately it is possible to investigate how changes in temperature and food availability might affect an individual's maturation and reproduction and, through it, population viability. For further details on the subject of population-level effects, the reader is referred to Section 8.5.

8.3. Tracking formation of metabolic products

Products in DEB can appear as a consequence of changes in stoichiometry when materials are transformed from one pool of materials into another. If the two pools have different stoichiometric composition, there must be excess material during the transformation corresponding to the difference. The law of conservation of mass implies that either the stoichiometric compositions of the pools have to change as the excess is returned to one or both pools, or that the materials need to be excreted in the form of a (metabolic) product. Since the strong homeostasis assumption requires that the compositions of the pools remain (near-)constant, product excretion is the only remaining option.

While many products are simply excreted into the environment, some are retained within the organism. The retained product can be recognized by its metabolic role. If it does not require maintenance, it is not structure; if it cannot be metabolized, it is not reserve; thus, it is a DEB product. Because the products are created in conjunction with active metabolic processes, consistency in

DEB require that they be expressed as a weighted sum of the three fundamental transformations (assimilation, growth, and dissipation). Furthermore, the law of conservation of mass requires that the functional dependence of contribution of each flux be linear: only a fixed proportion of any given flux is 'excess' and can contribute to product formation.

Cellulose that form tree trunks and otoliths in fish are examples of useful, retained DEB products. Cellulose is a complex carbohydrate that (among other functions) provides structural stability to green plants. Indeed, when integrated into a trunk, it neither requires maintenance, nor can it be used as a source of energy by the tree.

The same rules apply to fish otoliths, calcified structures in the fish inner ear whose growth and opacity depends on both fish metabolism (growth and other metabolic functions) and environmental conditions and, therefore, can exhibits seasonal variations in temperate environments. Otoliths can be assumed to be products in DEB theory because, even though they help with balance, orientation, and sound detection, they are metabolically inert. Moreover, because they grow even after the fish stops (as expected from a product not exclusively related to growth), otoliths provide a historical record of fish life history and environmental conditions experienced by the individual fish. Understanding this record, however, has been challenging; populations in apparently similar conditions can have widely different opacity patterns. The otoliths are difficult to interpret because it is difficult to disentangle the different factors that control opacity; for example, both high temperature and low growth conditions in winter can generate translucent sections. Modelling explicitly otolith growth *and* otolith opacity as functions of metabolic fluxes and temperature conditions can help us disentangle these drivers, get a more precise reconstruction of the growth pattern, and reconstruct a new variable: the amount of food assimilated.

Fablet et al. [158] and Pecquerie et al. [159] developed a comprehensive model of otolith growth based in DEB theory, and used it to analyze non-standard patterns of otolith growth in two cod populations (Barents Sea and the southern North Sea). Their research on biology of otoliths and cod identified (i) two fractions in the otoliths: a dark organic matrix, P, and a translucent mineral (aragonite) fraction, C, (ii) temperature dependence of aragonite precipitation, and (iii) two possible major contributions to otolith formation: growth and maintenance. Since otolith production is a weighted sums of the two contributions, they define

$$\frac{dV_P}{dt} = \alpha_P p_G + \beta_P p_M, \tag{36}$$

$$\frac{dV_C}{dt} = f(T)\left(\alpha_C p_G + \beta_C p_M\right), \tag{37}$$

where α_P and β_P are production weights for the organic matrix, α_C and β_C the production weights for the mineral fraction, and $f(T)$ is the temperature dependence of precipitation. Opacity is then given by the ratio of the two product functions.

First, parameters were fitted using independent data from experiments that had very different conditions from what could be expected in nature (one set with constant food level, another with nearly constant temperature). Next, the model was simulated with environmental conditions expected for the two natural cod populations. The simulated size and opacity of otoliths were markedly similar to real-life otoliths, and captured all details and differences between the two populations (Figure 6). Back-calculation using the DEB model (Figure 7) was also successful:

the back-calculated environmental conditions corresponded well with feeding and temperature in controlled experiments [159].

The generality of DEB implies that, once tested, the otolith model can be used for all similar processes, including shell growth in shellfish. More importantly, additional effects can be included, e.g., reduced biomineralization of calcium carbonate due to increase in CO_2, thus giving plausible predictions of biological effects for multiple climate scenarios based on readily available data. The ability to utilize multiple sources of information and decouple effects of multiple causes to correctly predict growth and reproduction of, as well as product formation by organisms in never before experienced environments is one of the chief benefits of DEB models, crucial for understanding future anthropogenic effects on individuals.

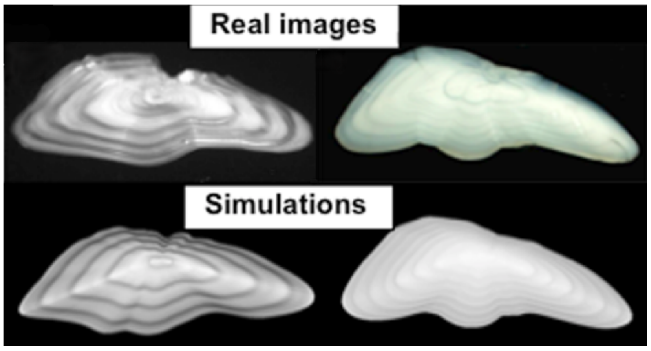

Figure 6: **Comparison of real and simulated otoliths.** Left: real (top) and simulated (bottom) otoliths from the southern North Sea population. Right: real (top) and simulated Barents Sea population (bottom). Note that only temperature and food forcing differ between the two populations; the model and parameter values are equal in both simulations. Adapted from Ref. [158].

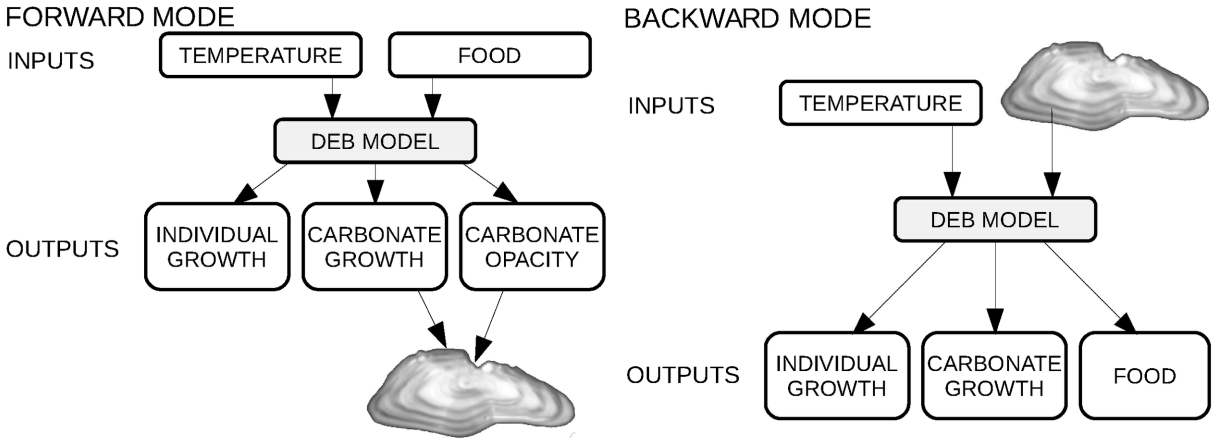

Figure 7: **Using DEB model to recover missing information.** Left plot ('forward mode'): DEB model is used to predict otolith growth and opacity from known temperature and food conditions. Right plot ('backward mode'): DEB model is used to predict otolith growth and food levels from known temperature and measurements of otolith opacity. Adapted from Ref. [159].

In addition to tracking formation of metabolic products, the rigorous definition of material

and energy fluxes in DEB enables tracking of incidental materials such as toxicants. The ability to quantitatively predict distribution of toxicants throughout the organism resulting from a given exposure is crucial to quantitative predictive ecotoxicology. Indeed, problems in ecotoxicology are historically responsible for the creation of the DEB theory.

8.4. Ecotoxicology

Traditional standardized toxicity tests determine acceptable levels of adverse effects, ECx, where EC stands for 'effective concentration', and x for the percentage of population exhibiting the investigated adverse effect. The ECx and older standard, no-effect concentration (NOEC) have been proven inadequate (see [160] for a summary). In short, NOEC and ECx give information about consequences of exposure with ad-libitum food over a standardized period of an animal of a certain size; data, however, show that the consequences depend on a number of factors such as food availability, organism size and age, exposure duration, and many more. DEB-based approaches address the shortcomings of the NOEC and ECx testing, and are included in the new OECD guidance [161] as an alternative to traditional tests. Most notably, DEB theory has been successful in capturing and predicting toxic effects of mixtures for multiple endpoints over the whole life cycle (see [162, 163] for overview). The advances have been made possible by the rigorous consideration of energy and material fluxes in DEB models.

DEB model fluxes not only determine growth and reproduction of individuals, but also their interaction with the environment, including toxicant intake with food, and assimilation of the toxicant through surfaces (e.g., skin). The energy and material fluxes within the organism specified by DEB also serve as a basis for determining how the toxicants distribute within the organism. The model linking the outside toxicant concentration with the internal bioaccumulation and distribution of the toxicant is called a *toxicokinetic* model. The results of the toxicokinetic model serve as an input to a *toxicodynamic* model that accounts for the effects of toxicants, and the resulting model can be incorporated into a population model (see [164] for a comprehensive review of population models suitable for this purpose).

Because DEB models capture all aspects of energy utilization, toxicodynamics (effects of the bioaccumulated toxicant) can be represented as effects on DEB parameters. In most applications, one or more DEB parameter values increase linearly with bioaccumulated toxicant density less some no-effect concentration, which represents the capacity of the organism to mitigate toxic effects (for a list of more than 70 relevant publications see [165]). While the standard DEB-based toxicology modeling (DEBtox) as described in Ref. [7] has a steep learning curve and may require a significant number of parameters, it more than compensates by providing numerous advantages over purely empirical modeling, most importantly:

- Multiple endpoints can be integrated independently and consistently.
- Modular construction: starting with the standard DEB model, modules can be attached as required by the research question, physiology of the organism, and/or environmental characteristics.
- Built-in constraints dictated by the physiology and strict observance to laws of physics help identify processes that govern responses to environmental conditions.

- Each set of measurements can be used to fit a disjointed set of parameters. For example, estimation of parameters governing the growth of zero-exposure treatment can be independent from estimation of parameters governing responses to toxicants.

- Parameter estimates for physiologically similar species estimated in completely different environments can be used to great effect, thereby drastically reducing data requirements; this is especially useful for species where experiments are impractical or illegal, and data are sparse and unevenly distributed (e.g., whales [166]).

- Once created and parameterized, a DEB-based model can give new insights into physiology by evaluating competing hypothesis.

Sometimes, the complexity of a toxicity model based on the full DEB model is not required for a specific task, and creates a 'barrier to entry' that prevents wider adoption and application of the theory. For these cases, Jager et al. [167] developed DEBkiss, a simplification of the standard DEB model.

DEBkiss simplifies the standard DEB by removing the energy reserve dynamics and assuming a constant body size at puberty. These simplifications remove maturity as a state variable, but the maturity maintenance can still be included. DEBkiss captures most of the nuances of the standard DEB, and is especially appropriate for small animals with small energy reserves, where parameters governing the reserve dynamics are difficult to estimate. Embryonic development, sustained by a dynamic reserve compartment in standard DEB, is in DEBkiss sustained by a buffer of assimilates in the egg, with egg weight as the primary parameter; the embryo hatches when the buffer runs out. As testified by more than a dozen DEBkiss papers since its inception in 2013, DEBkiss *significantly* simplifies the toxicity analysis because it uses less parameters, fewer state variables, and is easier to expand with toxicokinetic models.

DEBkiss (like other) simplifications, however, come at the cost of loss of generality. For example, DEBkiss parameters are not directly comparable to standard DEB model parameters, cannot be included in the Add_my_pet database, and special attention has to be used when comparing DEBkiss parameter values between species. Furthermore, when the environment is rapidly varying (compared to timescale of reserve equilibration in standard DEB), and/or size is not a good predictor of puberty, DEBkiss may skew predictions. Since population dynamics is especially susceptible to predictions determining fecundity (affected, among other factors, by timing of puberty), special attention should be paid when using DEBkiss to model populations in varying environments.

8.5. Population-level analysis

DEB, respecting the fundamentals of thermodynamics, relates biochemical level to the individual level of biological organization, but ecological applications require understanding of population-level dynamics. The understanding is especially important in the light of anthropogenic influence on the ecosystem (including global warming) because of a completely new set of environmental conditions developing at an unprecedented rate. Due to the rapid change of environmental conditions, species have to adapt without benefits of long-term individual adaptation through evolution. The population-level adaptations are reflected in changes of the size and age structure,

and patterns of growth and reproduction. Understanding and predicting these changes and patterns is crucial to our ability to properly account for limits of population-level adaptations in environmental management efforts such as species conservation, habitat preservation, and fishing rules and quotas. For example, predictions of changes in maturation size and age of a commercial fish species can help change fishing gear regulations years in advance, allowing for timely gear replacement. Without predictions, management reactions can only be retroactive: only once overfishing is noticeable, can rules and regulations change; by the time the changes are implemented in the field, it may already be too late. Empirical models could provide the needed information, but depend on experimental data. Population-level experiments, however, require multiple generations. Multi-generation experiments can take too long, be too expensive, and raise ethicsl concerns.

Population dynamics models making use of the ability of DEB models to predict individual growth and reproduction patterns offer a unique tool for providing quick and useful predictions. DEB models have successfully been incorporated into models of population dynamics: individual-based population models (IBMs) run the DEB model for each individual or group of individuals separately, while other approaches rely (e.g., matrix population models [168]) on simplifications and/or mean-field approximations.

All of the population-level models need to account for mortality. Mortality can be intrinsic, due to internal failures caused by starvation, aging and other sources of internal damage, or external due to external factors such as harvesting and predation. Only the basic ideas of aging in DEB are covered here; the reader is directed to Chapter 6 of Ref. [7] and Ref. [169] for details on aging in DEB, and numerous literature for accounting for other sources of mortality (e.g., [170, 171]).

Aging in DEB is assumed to be the consequence of accumulation of minute units of irreparable damage resulting from energy utilization. Oxidation required for energy utilization is extremely dangerous because oxidation of cellular components destroys their function. Cells have developed mechanisms to defend against the unwanted oxidation, but the defenses are not perfect, and some components do get damaged. Much of the damage can be repaired, but some damage to genetic information cannot be. Cellular components and functions based on the faulty genetic information have reduced efficiency, and are less able to defend against new damage, thus creating a positive feedback leading to accelerating accumulation of damage with a source term proportional to the energy utilization rate. Damage creates hazard, h, and the aging-induced mortality rate is assumed to be proportional to the hazard: probability of an organism alive at time t to be dead at $t + dt$ is equal to hdt. Toxicants can affect the hazard rate, as well as other cellular processes. Note that organisms in the wild rarely die of old age, and often the mortality due to aging can simply be ignored.

8.5.1. Individual-based models

IBMs have the most natural link with DEB models [164], in large part because they require less mathematical expertise to implement, and offer great flexibility in the choice of physiological models [172]. Although utilized before (e.g., [172, 173]), DEB-based IBMs have only recently been generally and rigorously implemented [174]. The publicly available DEB-IBM model implemented in NetLogo by Martin et al. [174] can be used to investigate any of the hundreds of species for which DEB parameters are known [114]. The software also allows for spatial heterogeneity in food levels, with a probabilistic movement decision tree able to incorporate primitive behavioral

changes.

The ability of the DEB-based IBM to correctly predict population dynamics was tested on one of the most commonly researched animals in DEB—*Daphnia* [175]. The model was able to predict population growth rates and peak densities, but could not correctly capture the population decline without assuming increase in infant mortality for low food levels. The model with food-dependent infant mortality, however, was able to correctly predict both large and small amplitude cycles previously observed in *Daphnia* populations feeding on algae in a mesocosm. In addition to providing robust predictions of independent data, the model was able to serve as a test bed for modeling alternatives. For example, Martin et al. [175] were able to test the need to include energy reserves as a state variable. Results suggest that—as long as maintenance during starvation is paid from structural biomass, and mortality is linked to assimilation—energy reserves can be omitted. This finding supports the use of net production models as a basis for stage structured models discussed below.

8.5.2. Stage-structured models

Stage structured models are mainstays of ecology; basing them on DEB models enables process-based analysis of population dynamics, and mechanistic analysis of inter-dependencies between multiple trophic levels. Compared to IBMs, stage-structured models require significantly less computing power, are less sensitive to effects of cohorts, and are easier to include into ecological networks, but require simplifications of the underlying DEB model. Furthermore, while using a stage-structure model, we gain the expediency of running the population model, but loose the ability to rigorously track material fluxes, as well as interrelate species by using scaling rules emanating from the full DEB description.

DEB-based stage-structured models include a number of simplifications, but can capture the general dynamics well regardless. For example, Nisbet et al. [176] use a net production model (in many respect similar to DEBkiss) to calculate functionals in delay-differential equations of the population dynamics model. The net production model includes only structure, W, and egg production, R, as state variables. The complexities of DEB growth dynamics are reduced by considering the production flux, $P = \kappa_A \dot{p}_A - \dot{p}_J - \dot{p}_M$. The production flux is responsible for all energy utilization towards growth and reproduction; the slowdown of growth and increase in production intrinsic to the full DEB model are captured by an assumed size-dependent allocation to growth, Θ:

$$\frac{dW}{dt} = \Theta P, \tag{38}$$

$$\frac{dR}{dt} = \frac{1}{w_e}(1-\Theta)P, \tag{39}$$

where w_e denotes units of energy required per egg. The simplified model was then used to drive population dynamics, and the feedbacks of food ingestion onto food availability (X). The resulting dynamics captured and offered insights into the previously investigated small- and large-amplitude cycles in *Daphnia* microcosms. Interplay between resource and population dynamics producing the oscillations in *Daphnia* populations is at the heart of many ecological questions.

Ananthasubramaniam et al. [177] take yet another approach. After assembling data from a large number of studies on *Daphnia magna*, they create a variant of a DEB model that captures specificities of the *Daphnia*, including molting. In addition to evaluating the DEB parameters, they calculate population growth rate for exposures at different food levels. Their subsequent sensitivity analysis was presented using heat maps, making the analysis conducive to the type of reasoning used in genomics and proteomics. They use the approach to cross-relate known omics data to the DEB analysis, thus identifying potential hotspots of toxicity response. Conceptually, the approach could be used to identify physiological roles of upregulated genes (and proteins): correlation between changes in DEB parameters describing a physiological process (e.g., assimilation) and upregulation of certain set of proteins suggests that the particular set is related to the physiological process.

8.5.3. Using DEB to directly model (bacterial) population growth and effects of toxicants

Populations of a special class of organisms, V1-morphs, can be modeled using the individual DEB model. V1-morphs are organisms whose surface area is proportional to volume for all sizes (e.g., filamentous hyphae of a fungus with a fixed diameter but variable length), signifying that all fluxes are proportional to volume. This, in turn, implies self-similarity: fluxes can be easily scaled to any size of the organism because ratios of fluxes are independent of size, so any part of the organism is representative of the whole. If appropriations to reproduction are also not size-, age-, or stage-dependent, organisms of all sizes contribute equally to the reproduction (normalized to size). Consequently, the same equations describe growth and reproduction normalized to size for any individual. If the simulated size is the sum of individual sizes of all organisms in the population, the equations describe population dynamics.

Microorganisms are small enough that, even though they may not be V1-morphs, their surface areas are proportional enough to their structural volumes that a V1-morph approximation can be made. Furthermore, there is often no distinction between growth and reproduction in microorganisms, and even if there is, the large numbers allow a mean-field approximation of energy commitment to reproduction. Therefore, microorganisms are prime targets for using DEB to directly model population growth. This is especially useful in ecotoxicology, where microorganisms are often the organisms of choice.

For example, the model of cadmium-ion toxicity on a bacteria, *P. aeruginosa* [178] uses a DEB model to model bacterial population growth and toxicokinetics. Rather than directly modifying the hazard rate, toxicodynamics is modeled by increasing the rate of damage created in the DEB aging module in proportion to the bioaccumulated toxicant. The greater rate of accumulation of damage leads to increase in hazard and, therefore, mortality. The inability to capture *P. aeruginosa* population-level responses from effects on mortality alone, indicated that additional toxicodynamic effects must be in play. Toxic effects on the maximum assimilation rate, and on acclimation (energy spent re-purposing the molecular machinery to reduce effects of exposure) were identified as the likely culprits. The resulting model was able to, using information on population dynamics in low toxicant concentrations, satisfactorily predict population-level responses to high toxicant concentrations (Fig. 8).

The mechanistic nature of DEB models makes them useful in verification of hypotheses, and enables self-consistent model expansion and inclusion of completely different data into the analy-

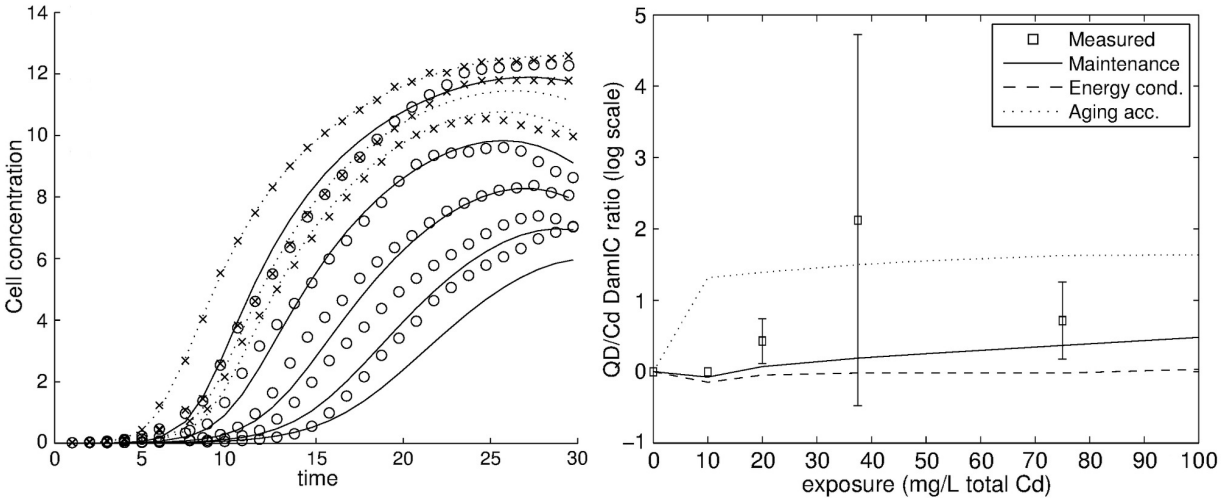

Figure 8: **Cadmium toxicity.** Left panel (adapted from Ref. [178]): predictions of the model for ionic toxicity. The model reproduces growth patterns for all treatments with a single common parameter set. Fitting toxicity parameters using bacterial growth for exposures of 0, 10, and 20 mg(Cd)/L (dotted lines) predicts well growth at exposures of up to 150 mg(Cd)/L well (solid lines). Right panel (adapted from Ref. [179]): predictions of damage-inducing compound (DamIC) levels (lines) compared to ROS levels (squares) for three different toxicodynamic modes: increase in costs of maintenance (solid line), decrease in energy conductance (dashed line), and increase in negative effects of previous damage (aging acceleration, dotted line). Increase in maintenance costs results in a pattern of damage-inducing compounds most like the observed ROS pattern.

sis. For example, Klanjscek et al. [179] used the ionic model of Cd toxicity to test and disprove the hypothesis that ionic toxicity could be responsible for toxicity of cadmium-selenium quantum dots (CdSe QDs), an engineered nanomaterial. Next, they expanded the model to include toxicokinetics and toxicodynamics of the QDs, while keeping all parameter values from the ionic part of the model unchanged. Because any and all metabolic processes could have been affected, the authors tested a number of alternatives. The growth curves lead to conclusions that—unlike the ionic toxicity—acclimation to nano-toxicity requires energy investment that increases with exposure. Also, additional data on abundance of reactive oxygen species (ROS) helped identify increase in maintenance due to bioaccumulated QDs as the most likely propagator of the toxicodynamic effect.

The few examples presented in this section represent neither the typical, nor the extent of possible uses of the DEB theory; for the most part, they focus on the non-standard approaches to DEB. Apart from avoiding having to choose among many excellent DEB applications, this is to make the point that DEB theory goes beyond the description of all life forms: it provides a comprehensive, highly adaptable platform for investigating causal links between objects and actors on all levels of biological organization, starting with molecular dynamics, through individuals and populations, to the ecosystem (see also [8]). DEB is unique in its ability to predict effects of alternative environmental scenarios on organisms, thus offering a way to inform decision-makers and enable proactive policies necessary to successfully adapt to, and mitigate effects of, environmental pollution and oncoming global climate change. This will be especially important in the new, Anthropocene era where our actions are the main drivers of change on the planet Earth, and we no

longer have the luxury of experimenting with the ecosystem.

Acknowledgements

We would also like to thank L. Pecquerie, B. Martin, R.M. Nisbet, E. Zimmer, and T. Jager for help with reviewing parts of the manuscript. This work has been in part supported by the Japan Science and Technology Agency (JST) Program to Disseminate Tenure Tracking System, the United States National Science Foundation (US NSF) and the United States Environmental Protection Agency (US EPA) under Cooperative Agreement #EF-0830117, and the Croatian Science Foundation under project 2202-ACCTA.

A. Summary of key equations and quantities

To provide a complete overview of the standard DEB model in one place, here follows a summary of key equations and quantities. The model dynamics covering the development of an organism from an egg to a fully mature adult are given by

$$\frac{dE}{dt} = \dot{p}_A - \dot{p}_C, \qquad \text{Reserve dynamics}$$

$$\frac{dL}{dt} = \frac{\dot{p}_G}{3L^2\,[E_G]}, \quad \text{and} \qquad \text{Growth}$$

$$\frac{dE_H}{dt} = \begin{cases} \dot{p}_R, & \text{if } \; E_H < E_H^p \\ 0, & \text{if } \; E_H = E_H^p \end{cases}. \qquad \text{Maturation}$$

For these ordinary differential equations to be solvable, energy flows should be specified in terms of the state variables

$$\dot{p}_A = \begin{cases} 0, & \text{if } \; E_H < E_H^b \\ \{\dot{p}_{Am}\}\, f L^2, & \text{otherwise} \end{cases} \qquad \text{Assimilation}$$

$$\dot{p}_C = [E]\,\frac{\dot{v}\,[E_G]\,L^2 + [\dot{p}_M]\,L^3 + \{\dot{p}_T\}\,L^2}{[E_G] + \kappa\,[E]}, \qquad \text{Utilization}$$

$$\dot{p}_G = [E_G]\,\frac{\kappa\dot{v}\,[E]\,L^2 - [\dot{p}_M]\,L^3 - \{\dot{p}_T\}L^2}{[E_G] + \kappa\,[E]}, \quad \text{and} \qquad \text{Growth}$$

$$\dot{p}_R = (1-\kappa)\,\dot{p}_C - \dot{k}_J E_H. \qquad \text{Maturation}$$

Important symbols appearing in the model equations are conveniently summarized in Table A.1.

To close the life cycle of an organism, an estimate of the reproductive output is still needed. The rate of continuous egg production, for example, is estimable using

$$\dot{R} = \frac{\kappa_R}{E_0} \times \begin{cases} 0, & \text{if } \; E_H < E_H^p \\ \dot{p}_R, & \text{if } \; E_H = E_H^p \end{cases}. \qquad \text{Egg production rate}$$

An alternative to continuous egg production is intermittent reproduction limited to a suitable window of opportunity called the reproductive season. Between two consecutive reproductive seasons, energy allocated to reproduction is stored in a buffer according to

$$\frac{dE_R}{dt} = \begin{cases} 0, & \text{if } \; E_H < E_H^p \\ \dot{p}_R, & \text{if } \; E_H = E_H^p \end{cases}. \qquad \text{Reproduction buffer}$$

Obtaining the rate of intermittent egg production from energy in the reproduction buffer requires defining species-specific buffer handling rules.

Although not strictly necessary from a mathematical perspective, in some applications (e.g., ecotoxicology), it is useful to explicitly write down the two maintenance flows as

$$\dot{p}_S = [\dot{p}_M]\,L^3 + \{\dot{p}_T\}\,L^2, \quad \text{and} \qquad \text{Somatic maint.}$$

$$\dot{p}_J = \dot{k}_J E_H, \qquad \text{Maturity maint.}$$

which can then be used to slightly simplify the equations for other flows, i.e., utilization, growth, and maturation. The reason for doing such a simplification and emphasizing the role of maintenance flows is that some toxicants, e.g., xenobiotics, directly influence the value of maintenance-related parameters. Instead of having an environmental effect on the parameter values scattered across multiple model equations, it is usually a better practice to capture these changes in a single equation whenever possible.

One more equation consistently used in conjunction with the standard DEB model is the Arrhenius relationship. This relationship captures the effect of temperature on the metabolic rates of ectotherms

$$\dot{p}_*(T) = \dot{p}_*(T_{ref}) \exp\left(\frac{T_A}{T_{ref}} - \frac{T_A}{T}\right). \qquad \text{Arrhenius rel.}$$

When additionally the temperature tolerance range of an ectothermic organism needs to be accounted for, the Arrhenius relationship is extendable by multiplying its right-hand side by ratio $\gamma(T_{ref})/\gamma(T)$, where function $\gamma = \gamma(T)$ is given in Eq. (2).

Table A.1: Key quantities appearing in the standard DEB model.

Symbol	Description	Unit
$E(t)$	Energy in reserve	J
$L(t)$	Structural length	cm
$E_H(t)$	Level of maturity	J
$E_R(t)$	State of the reproduction buffer	J
E_0	Initial energy reserve of an egg	J
$f(t)$	Scaled functional response (see Section 6.2)	–
T	Body temperature	K
$\{\dot{p}_{Am}\}$	Maximum surface-area-specific assimilation rate	$\mathrm{J\,d^{-1}\,cm^{-2}}$
$\dot{v}$	Energy conductance	$\mathrm{cm\,d^{-1}}$
κ	Allocation fraction to soma	–
κ_R	Reproduction efficiency	–
$[\dot{p}_M]$	Volume-specific somatic maintenance cost	$\mathrm{J\,d^{-1}\,cm^{-3}}$
$\{\dot{p}_T\}$	Surface-area-specific somatic maintenance cost	$\mathrm{J\,d^{-1}\,cm^{-2}}$
$\dot{k}_J$	Maturity maintenance rate coefficient	$\mathrm{d^{-1}}$
$[E_G]$	Volume-specific cost of structure	$\mathrm{J\,cm^{-3}}$
E_H^b	Maturity at birth	J
E_H^p	Maturity at puberty	J
T_A	Arrhenius temperature	K
T_{ref}	Reference body temperature for parameter values	K

B. Embryonic development and the initial conditions

In DEB theory, an egg is assumed to initially contain only reserve received from the mother. By utilizing this reserve the embryo develops until becoming capable of feeding on its own. Under

such conditions, as shown in Section 6.5, the triplet of the scaled state variables (e, l, e_H) at scaled time $\tau = 0$ is $\left(+\infty, 0, e_H^0\right)$, where $e_H^0 = (1-\kappa)\, g$. Because the embryo is not feeding on an outside food source, the scaled energy density is decreasing until it reaches value e_b at the moment of first feeding (i.e., birth in DEB terminology because the first feeding represents a major shift in the energy budget of any organism). The value of the scaled reserve density at birth is assumed to be known due to the maternal effect [110]. Namely, $e_b = f$, where f is food availability experienced by the mother. These considerations indicate that the scaled reserve density is a monotonically decreasing function of time (from $e = +\infty$ initially to $e = e_b$ at birth), thus allowing us to simplify the system of Eqs. (32) and (33) by using e as an independent variable instead of scaled time τ. We get an ordinary differential equation

$$\frac{dl}{de} = -\frac{l}{3e}\frac{e-l}{e+g}, \tag{B.1}$$

where we have taken into account that embryos do not feed ($f = 0$) and have negligible surface-area related somatic maintenance costs ($l_T = 0$).

Eq. (B.1) has an exact solution

$$l(e) = \frac{2g}{-2 + 2Cg^{4/3}\,(1+e/g)^{1/3} + (1+e/g)\,\Re\left[{}_2F_1\left(2/3, 1, 5/3, 1+e/g\right)\right]}, \tag{B.2}$$

where C is an unknown integration constant, $\Re$ is the real part of a complex number, and ${}_2F_1(\cdot,\cdot,\cdot,\cdot)$ is a hypergeometric function. The correctness of this solution can be proven by inserting Eq. (B.2) back to Eq. (B.1). More importantly, we see that determining the integration constant C is equivalent to determining scaled length at birth, l_b, because $l_b = l(e_b)$, which can be solved for l_b when C is known and vice versa. Function $l(e)$ can be slightly simplified by substituting $x = 1 + e/g$, which runs from $x_0 = +\infty$ to $x_b = 1 + e_b/g$ during the course of embryonic development.

Constant C is constrained by Eq. (35) for the scaled maturity density. However, the problem is considerably simplified if we substitute $h = l^3 e_H/(1-\kappa)$, upon which maturity is tracked with equation

$$\frac{dh}{dx} = \frac{k}{g}\frac{l(x)}{x-1}h(x) - [l(x)]^3\,\frac{l(x)+g}{x}, \tag{B.3}$$

where $h(x_0) = 0$ and $h(x_b) = l_b^3 e_H^b/(1-\kappa)$—a known value because $l_b^3 e_H^b = E_H^b/([E_m]\,L_m^3)$. Eq. (B.3) is recognizable as a first-order linear differential equation of the form $\frac{dh}{dx} + P(x)\,h = Q(x)$ [180]. In our case, $P(x) = -\frac{k}{g}\frac{l(x)}{x-1}$ and $Q(x) = -[l(x)]^3\,\frac{l(x)+g}{x}$. The general solution is [180]

$$h(x) = \exp\left(-\int_{x_b}^{x} P(x')\,dx'\right) \times \left[h(x_b) + \int_{x_b}^{x} Q(x')\exp\left(\int_{x_b}^{x'} P(x'')\,dx''\right)dx'\right]. \tag{B.4}$$

Fortunately, we do not need to solve this equation to find the value of constant C. Instead, it is sufficient to use the fact that $h(x_0) = 0$, yielding

$$h(x_b) = -\int_{x_b}^{x_0} Q(x')\exp\left(\int_{x_b}^{x'} P(x'')\,dx''\right)dx'. \tag{B.5}$$

From this condition, constant C is readily calculated using numerical integration. Once the value of C is known, the initial condition for simulating post-embryonic development with the standard DEB model is $\left(e_b, l_b(e_b), e_H^b\right)$.

If constant C is known, can it be used to calculate the initial energy reserve of an egg, E_0? The answer is affirmative, and the relationship to perform this calculation is

$$E_0 = \frac{[E_m]\, L_m^3}{\left(C - \frac{1}{4}\Gamma\left(\frac{1}{3}\right)\Gamma\left(\frac{5}{3}\right)\right)^3}, \tag{B.6}$$

where $\Gamma(\cdot)$ is the gamma function. Proving Eq. (B.6) is quite technical and laborious, and hence omitted here. Fortunately, it is possible to test its correctness numerically against an equivalent relationship [110] (see also Section 2.6 in [7]). Given the numerical example in Fig. 3 with $\kappa = 0.8$, $E_H^b = 7.425\,\mathrm{J}$, and $k \approx 0.9333$ at $e_b = f = 0.8$, we obtain $C = 12.5497$. This value for C gives $l_b = 0.05075$ and $E_0 = 47.6\,\mathrm{J}$, which are precisely the expected results.

References

[1] N. Bellomo, A. Elaiw, A. M. Althiabi, M. A. Alghamdi, On the interplay between mathematics and biology: Hallmarks toward a new systems biology, Phys. Life Rev. 12 (2015) 44–64.

[2] J. E. Cohen, Mathematics is biology's next microscope, only better; biology is mathematics' next physics, only better, PLOS Biol. 2 (2004) e439.

[3] M. Gruebele, D. Thirumalai, Perspective: Reaches of chemical physics in biology, J. Chem. Phys. 139 (2013) 121701.

[4] X. Wu, P. G. Schultz, Synthesis at the interface of chemistry and biology, J. Am. Chem. Soc. 131 (2009) 12497–12515.

[5] A. Rau, Biological scaling and physics, J. Biosci. 27 (2002) 475–478.

[6] L. von Bertalanffy, The theory of open systems in physics and biology, Science 111 (1950) 23–29.

[7] S. A. L. M. Kooijman, Dynamic Energy Budget theory for metabolic organisation, Cambridge University Press, 2010.

[8] R. Nisbet, E. Muller, K. Lika, S. A. L. M. Kooijman, From molecules to ecosystems through Dynamic Energy Budget models, J. Anim. Ecol. 69 (2000) 913–926.

[9] J. van der Meer, C. Klok, M. R. Kearney, J. W. Wijsman, S. A. L. M. Kooijman, 35 years of DEB research, J. Sea Res. 94 (2014) 1–4.

[10] T. Sousa, T. Domingos, S. A. L. M. Kooijman, From empirical patterns to theory: A formal metabolic theory of life, Phil. Trans. R. Soc. B 363 (2008) 2453–2464.

[11] T. Sousa, T. Domingos, J.-C. Poggiale, S. A. L. M. Kooijman, Dynamic Energy Budget theory restores coherence in biology, Phil. Trans. R. Soc. B 365 (2010) 3413–3428.

[12] T. Sousa, R. Mota, T. Domingos, S. A. L. M. Kooijman, Thermodynamics of organisms in the context of Dynamic Energy Budget theory, Phys. Rev. E 74 (2006) 051901.

[13] R. M. Nisbet, M. Jusup, T. Klanjscek, L. Pecquerie, Integrating Dynamic Energy Budget (deb) theory with traditional bioenergetic models, J. Exp. Biol. 215 (2012) 892–902.

[14] S. C. Woods, R. J. Seeley, D. Porte, M. W. Schwartz, Signals that regulate food intake and energy homeostasis, Science 280 (1998) 1378–1383.

[15] R. W. Sterner, J. J. Elser, Ecological stoichiometry: The biology of elements from molecules to the biosphere, Princeton University Press, 2002.

[16] R. Albert, Scale-free networks in cell biology, J. Cell Sci. 118 (2005) 4947–4957.

[17] H. Jeong, B. Tombor, R. Albert, Z. N. Oltvai, A.-L. Barabási, The large-scale organization of metabolic networks, Nature 407 (2000) 651–654.

[18] G. Robinson, R. W. Butcher, E. W. Sutherland, Cyclic AMP, Academic Press, 1971.

[19] G. Robinson, R. W. Butcher, E. W. Sutherland, Cyclic AMP, Annu. Rev. Biochem. 37 (1968) 149–174.

[20] D. A. Walsh, S. M. Van Patten, Multiple pathway signal transduction by the cAMP-dependent protein kinase, FASEB J. 8 (1994) 1227–1236.

[21] E. R. Kandel, The molecular biology of memory storage: a dialogue between genes and synapses, Science 294 (2001) 1030–1038.

[22] E. Ferrannini, The theoretical bases of indirect calorimetry: A review, Metabolism 37 (1988) 287–301.

[23] H. A. Haugen, L.-N. Chan, F. Li, Indirect calorimetry: A practical guide for clinicians, Nutr. Clin. Pract. 22 (2007) 377–388.

[24] B. Kégl, Intrinsic dimension estimation using packing numbers, in: Advances in neural information processing systems, pp. 681–688.

[25] E. Levina, P. J. Bickel, Maximum likelihood estimation of intrinsic dimension, in: Advances in neural information processing systems, pp. 777–784.

[26] F. Y. Kuo, I. H. Sloan, Lifting the curse of dimensionality, Notices Amer. Math. Soc. 52 (2005) 1320–1328.

[27] M. Verleysen, D. François, The curse of dimensionality in data mining and time series prediction, in: Computational Intelligence and Bioinspired Systems, Springer, 2005, pp. 758–770.

[28] V. Winschel, M. Krätzig, Solving, estimating, and selecting nonlinear dynamic models without the curse of dimensionality, Econometrica 78 (2010) 803–821.

[29] J. Annan, J. Hargreaves, N. Edwards, R. Marsh, Parameter estimation in an intermediate complexity earth system model using an ensemble Kalman filter, Ocean Model. 8 (2005) 135–154.
[30] M. A. Beaumont, Approximate Bayesian computation in evolution and ecology, Annu. Rev. Ecol. Evol. Syst. 41 (2010) 1.
[31] Z. Wang, M. A. Andrews, Z.-X. Wu, L. Wang, C. T. Bauch, Coupled disease–behavior dynamics on complex networks: A review, Phys. Life Rev. 15 (2015) 1–29.
[32] M. Jusup, S. Iwami, B. Podobnik, H. E. Stanley, Dynamically rich, yet parameter-sparse models for spatial epidemiology. Comment on "Coupled disease-behavior dynamics on complex networks: A review" by Z. Wang et al., Phys. Life Rev. 15 (2015) 43–46.
[33] M. Fujiwara, B. E. Kendall, R. M. Nisbet, W. A. Bennett, Analysis of size trajectory data using an energetic-based growth model, Ecology 86 (2005) 1441–1451.
[34] J. van der Meer, An introduction to Dynamic Energy Budget (DEB) models with special emphasis on parameter estimation, J. Sea Res. 56 (2006) 85–102.
[35] S. A. L. M. Kooijman, T. Sousa, L. Pecquerie, J. Van der Meer, T. Jager, From food-dependent statistics to metabolic parameters, a practical guide to the use of dynamic energy budget theory, Biol. Rev. 83 (2008) 533–552.
[36] K. Lika, M. R. Kearney, V. Freitas, H. W. van der Veer, J. van der Meer, J. W. Wijsman, L. Pecquerie, S. A. L. M. Kooijman, The "covariation method" for estimating the parameters of the standard Dynamic Energy Budget model I: philosophy and approach, J. Sea Res. 66 (2011) 270–277.
[37] K. Lika, M. R. Kearney, S. A. L. M. Kooijman, The "covariation method" for estimating the parameters of the standard Dynamic Energy Budget model II: properties and preliminary patterns, J. Sea Res. 66 (2011) 278–288.
[38] L. R. Johnson, L. Pecquerie, R. M. Nisbet, Bayesian inference for bioenergetic models, Ecology 94 (2013) 882–894.
[39] K. Popper, The logic of scientific discovery, Routledge, 2005.
[40] J. H. Brown, J. F. Gillooly, A. P. Allen, V. M. Savage, G. B. West, Toward a metabolic theory of ecology, Ecology 85 (2004) 1771–1789.
[41] G. B. West, J. H. Brown, B. J. Enquist, A general model for the origin of allometric scaling laws in biology, Science 276 (1997) 122–126.
[42] J. L. Maino, M. R. Kearney, R. M. Nisbet, S. A. L. M. Kooijman, Reconciling theories for metabolic scaling, J. Anim. Ecol. 83 (2014) 20–29.
[43] J. van der Meer, Metabolic theories in ecology, Trends Ecol. Evol. 21 (2006) 136–140.
[44] N. J. Isaac, C. Carbone, Why are metabolic scaling exponents so controversial? Quantifying variance and testing hypotheses, Ecol. Lett. 13 (2010) 728–735.
[45] M. R. Kearney, C. R. White, Testing metabolic theories, Amer. Nat. 180 (2012) 546–565.
[46] C. A. Price, J. S. Weitz, V. M. Savage, J. Stegen, A. Clarke, D. A. Coomes, P. S. Dodds, R. S. Etienne, A. J. Kerkhoff, K. McCulloh, et al., Testing the metabolic theory of ecology, Ecol. Lett. 15 (2012) 1465–1474.
[47] M. D. Brand, Regulation analysis of energy metabolism., J. Exp. Biol. 200 (1997) 193–202.
[48] R. W. Sterner, N. B. George, Carbon, nitrogen, and phosphorus stoichiometry of cyprinid fishes, Ecology 81 (2000) 127–140.
[49] J. Persson, P. Fink, A. Goto, J. M. Hood, J. Jonas, S. Kato, To be or not to be what you eat: regulation of stoichiometric homeostasis among autotrophs and heterotrophs, Oikos 119 (2010) 741–751.
[50] K. Mulder, W. B. Bowden, Organismal stoichiometry and the adaptive advantage of variable nutrient use and production efficiency in *Daphnia*, Ecol. Model. 202 (2007) 427–440.
[51] B. Krasnov, I. Khokhlova, L. Fielden, N. Burdelova, Time of survival under starvation in two flea species (Siphonaptera: Pulicidae) at different air temperatures and relative humidities, J. Vector Ecol. 27 (2002) 70–81.
[52] B. A. Stockhoff, Starvation resistance of gypsy moth, *Lymantria dispar* (L.)(Lepidoptera: Lymantriidae): Tradeoffs among growth, body size, and survival, Oecologia 88 (1991) 422–429.
[53] H. Bilton, G. Robins, The effects of starvation and subsequent feeding on survival and growth of Fulton channel sockeye salmon fry (*Oncorhynchus nerka*), J. Fish. Res. Board Can. 30 (1973) 1–5.

[54] N. Wilkins, Starvation of the herring, *Clupea harengus* L.: Survival and some gross biochemical changes, Comp. Biochem. Phys. 23 (1967) 503–518.
[55] D. Montemurro, J. Stevenson, Survival and body composition of normal and hypothalamic obese rats in acute starvation, Am. J. Physiol. 198 (1960) 757–761.
[56] M. A. Vanderklift, S. Ponsard, Sources of variation in consumer-diet δ^{15}N enrichment: A meta-analysis, Oecologia 136 (2003) 169–182.
[57] C. E. Boyd, C. Tucker, A. McNevin, K. Bostick, J. Clay, Indicators of resource use efficiency and environmental performance in fish and crustacean aquaculture, Rev. Fish. Sci. 15 (2007) 327–360.
[58] B. Glencross, M. Booth, G. Allan, A feed is only as good as its ingredients–a review of ingredient evaluation strategies for aquaculture feeds, Aquacult. Nutr. 13 (2007) 17–34.
[59] K. P. Sebens, The ecology of indeterminate growth in animals, Annu. Rev. Ecol. Syst. 18 (1987) 371–407.
[60] M. Jusup, T. Klanjšček, H. Matsuda, Simple measurements reveal the feeding history, the onset of reproduction, and energy conversion efficiencies in captive bluefin tuna, J. Sea Res. 94 (2014) 144–155.
[61] S. J. Plaistow, C. T. Lapsley, A. P. Beckerman, T. G. Benton, Age and size at maturity: sex, environmental variability and developmental thresholds, Proc. R. Soc. B 271 (2004) 919–924.
[62] B. Merry, A. M. Holehan, Onset of puberty and duration of fertility in rats fed a restricted diet, J. Reprod. Fertil. 57 (1979) 253–259.
[63] S. Asdell, M. F. Crowell, The effect of retarded growth upon the sexual development of rats, J. Nutr. 10 (1935) 13–24.
[64] A. Hulbert, P. Else, Basal metabolic rate: history, composition, regulation, and usefulness, Physiol. Biochem. Zool. 77 (2004) 869–876.
[65] S. Logan, The origin and status of the Arrhenius equation, J. Chem. Educ 59 (1982) 279.
[66] P. J. Sharpe, D. W. DeMichele, Reaction kinetics of poikilotherm development, J. of Theor. Biol. 64 (1977) 649–670.
[67] A. Clarke, Is there a universal temperature dependence of metabolism?, Funct. Ecol. 18 (2004) 252–256.
[68] H. Hoppeler, E. R. Weibel, Scaling functions to body size: theories and facts, J. Exp. Biol. 208 (2005) 1573–1574.
[69] J. Whitfield, In the beat of a beart: Life, energy, and the unity of nature, Joseph Henry Press, 2006.
[70] P. A. Corning, S. J. Kline, Thermodynamics, information and life revisited, Part I: "To be or entropy", Syst. Res. Behav. Sci. 15 (1998) 273–295.
[71] L. Garby, P. S. Larsen, Bioenergetics—Its thermodynamic foundations, Cambridge University Press, 1995.
[72] N. P. Smith, C. J. Barclay, D. S. Loiselle, The efficiency of muscle contraction, Prog. Biophys. Mol. Biol. 88 (2005) 1–58.
[73] M. R. Kearney, A. Matzelle, B. Helmuth, Biomechanics meets the ecological niche: The importance of temporal data resolution, J. Exp. Biol. 215 (2012) 922–933.
[74] M. Kearney, R. Shine, W. P. Porter, The potential for behavioral thermoregulation to buffer "cold-blooded" animals against climate warming, Proc. Natl. Acad. Sci. U.S.A. 106 (2009) 3835–3840.
[75] E. H. Battley, An empirical method for estimating the entropy of formation and the absolute entropy of dried microbial biomass for use in studies on the thermodynamics of microbial growth, Thermochim. Acta 326 (1999) 7–15.
[76] N. Marn, T. Klanjscek, L. Stokes, M. Jusup, Size scaling in western north atlantic loggerhead turtles permits extrapolation between regions, but not life stages, PLOS ONE 10 (2015) e0143747.
[77] B. Mendes, P. Fonseca, A. Campos, Weight–length relationships for 46 fish species of the Portuguese west coast, J. Appl. Ichthyol. 20 (2004) 355–361.
[78] K. A. Bjorndal, A. B. Bolten, Growth rates of immature green turtles, *Chelonia mydas*, on feeding grounds in the southern Bahamas, Copeia (1988) 555–564.
[79] J. Forsythe, R. Hanlon, Effect of temperature on laboratory growth, reproduction and life span of *Octopus bimaculoides*, Mar. Biol. 98 (1988) 369–379.
[80] N. Daan, Growth of North Sea cod, *Gadus morhua*, Neth. J. Sea Res. 8 (1974) 27–48.
[81] S. A. L. M. Kooijman, Dynamic energy budgets in biology systems–theory and applications in ecotoxicology, Cambridge University Press, 1993.

[82] I. V. Hinkson, J. E. Elias, The dynamic state of protein turnover: It's about time, Trends Cell Biol. 21 (2011) 293–303.
[83] A. Quigg, J. Beardall, Protein turnover in relation to maintenance metabolism at low photon flux in two marine microalgae, Plant Cell Environ. 26 (2003) 693–703.
[84] K. Noguchi, C.-S. Go, S.-I. Miyazawa, I. Terashima, S. Ueda, T. Yoshinari, Costs of protein turnover and carbohydrate export in leaves of sun and shade species, Funct. Plant Biol. 28 (2001) 37–47.
[85] D. Houlihan, S. Hall, C. Gray, B. Noble, Growth rates and protein turnover in Atlantic cod, *Gadus morhua*, Can. J. Fish. Aquat. Sci. 45 (1988) 951–964.
[86] A. Hawkins, B. Bayne, A. Day, Protein turnover, physiological energetics and heterozygosity in the blue mussel, *Mytilus edulis*: the basis of variable age-specific growth, Proc. R. Soc. B 229 (1986) 161–176.
[87] A. G. Marsh, R. E. Maxson, D. T. Manahan, High macromolecular synthesis with low metabolic cost in antarctic sea urchin embryos, Science 291 (2001) 1950–1952.
[88] T. Bouma, R. D. Visser, J. Janssen, M. d. Kock, P. v. Leeuwen, H. Lambers, Respiratory energy requirements and rate of protein turnover *in vivo* determined by the use of an inhibitor of protein synthesis and a probe to assess its effect, Physiol. Plant. 92 (1994) 585–594.
[89] D. Houlihan, Protein turnover in ectotherms and its relationships to energetics, in: Advances in comparative and environmental physiology, Springer, 1991, pp. 1–43.
[90] Y. Aoyagi, I. Tasaki, J. Okumura, T. Muramatsu, Energy cost of whole-body protein synthesis measured in vivo in chicks, Comp. Biochem. Physiol. B–Biochem. Mol. Biol. 91 (1988) 765–768.
[91] J. Waterlow, Protein turnover with special reference to man, Q. J. Exp. Physiol. 69 (1984) 409–438.
[92] L. Von Bertalanffy, Quantitative laws in metabolism and growth, Q. Rev. Biol. (1957) 217–231.
[93] N. Lester, B. Shuter, P. Abrams, Interpreting the von Bertalanffy model of somatic growth in fishes: the cost of reproduction, Proc. R. Soc. B 271 (2004) 1625–1631.
[94] S. Ohnishi, T. Yamakawa, H. Okamura, T. Akamine, A note on the von Bertalanffy growth function concerning the allocation of surplus energy to reproduction, Fish. Bull. 110 (2012) 223–229.
[95] M. W. Schwartz, S. C. Woods, R. J. Seeley, G. S. Barsh, D. G. Baskin, R. L. Leibel, Is the energy homeostasis system inherently biased toward weight gain?, Diabetes 52 (2003) 232–238.
[96] K. G. Murphy, S. R. Bloom, Gut hormones and the regulation of energy homeostasis, Nature 444 (2006) 854–859.
[97] D. G. Hardie, F. A. Ross, S. A. Hawley, Ampk: a nutrient and energy sensor that maintains energy homeostasis, Nat. Rev. Mol. Cell Biol. 13 (2012) 251–262.
[98] A. C. Lloyd, The regulation of cell size, Cell 154 (2013) 1194–1205.
[99] A. J. Tessier, L. L. Henry, C. E. Goulden, M. W. Durand, Starvation in Daphnia: energy reserves and reproductive allocation, Limnol. Oceanogr. 28 (1983) 667–676.
[100] M. Yin, J. Blaxter, Feeding ability and survival during starvation of marine fish larvae reared in the laboratory, J. Exp. Mar. Biol. Ecol. 105 (1987) 73–83.
[101] A. Folkvord, Growth, survival and cannibalism of cod juveniles (*Gadus morhua*): effects of feed type, starvation and fish size, Aquaculture 97 (1991) 41–59.
[102] H. Briegel, I. Knusel, S. E. Timmermann, *Aedes aegypti*: size, reserves, survival, and flight potential, J. Vector Ecol. 26 (2001) 21–31.
[103] M. J. Couvillon, A. Dornhaus, Small worker bumble bees (*Bombus impatiens*) are hardier against starvation than their larger sisters, Insectes Soc. 57 (2010) 193–197.
[104] S. Augustine, M. Litvak, S. A. L. M. Kooijman, Stochastic feeding of fish larvae and their metabolic handling of starvation, J. Sea Res. 66 (2011) 411–418.
[105] C. J. Monaco, D. S. Wethey, B. Helmuth, A dynamic energy budget (DEB) model for the keystone predator *Pisaster ochraceus*, PLOS ONE 9 (2014) e104658.
[106] F. Richards, A flexible growth function for empirical use, J. Exp. Bot. 10 (1959) 290–301.
[107] A. J. Fabens, et al., Properties and fitting of the von Bertalanffy growth curve, Growth 29 (1965) 265–289.
[108] D. K. Kimura, Likelihood methods for the von Bertalanffy growth curve, Fish. Bull. 77 (1980) 765–776.
[109] Y. Chen, D. Jackson, H. Harvey, A comparison of von Bertalanffy and polynomial functions in modelling fish growth data, Can. J. Fish. Aquat. Sci. 49 (1992) 1228–1235.

[110] S. A. L. M. Kooijman, What the egg can tell about its hen: Embryonic development on the basis of dynamic energy budgets, J. Math. Biol. 58 (2009) 377–394.
[111] M. Kleiber, Body size and metabolism, Hilgardia 6 (1932) 315–345.
[112] P. S. Agutter, D. N. Wheatley, Metabolic scaling: consensus or controversy?, Theor. Biol. Med. Model. 1 (2004) 13.
[113] http://www.bio.vu.nl/thb/deb/DEB_papers.pdf, N/A. Accessed: 15-Aug-2016.
[114] Add_my_pet: species list, http://www.bio.vu.nl/thb/deb/deblab/add_my_pet/index_species.html, N/A. Accessed: 15-Aug-2016.
[115] S. A. L. M. Kooijman, Software package debtool, http://www.bio.vu.nl/thb/deb/deblab/debtool/DEBtool_M/manual/index.html, 2010. Accessed: 15-Aug-2016.
[116] C. M. G. L. Teixeira, Application of Dynamic Energy Budget theory for conservation relevant modelling of bird life histories, Ph.D. thesis, VU University Amsterdam & Lisbon University, 2016.
[117] S. A. L. M. Kooijman, K. Lika, Resource allocation to reproduction in animals, Biol. Rev. Camb. Philos. Soc. 89 (2014) 849–859.
[118] S. A. L. M. Kooijman, K. Lika, Comparative energetics of the 5 fish classes on the basis of dynamic energy budgets, J. Sea Res. 94 (2014) 19–28.
[119] S. A. L. M. Kooijman, L. Pecquerie, S. Augustine, M. Jusup, Scenarios for acceleration in fish development and the role of metamorphosis, Journal of Sea Research 66 (2011) 419–423.
[120] S. A. L. M. Kooijman, Metabolic acceleration in animal ontogeny: an evolutionary perspective, J. Sea Res. 94 (2014) 128–137.
[121] S. A. L. M. Kooijman, Waste to hurry: dynamic energy budgets explain the need of wasting to fully exploit blooming resources, Oikos 122 (2013) 348–357.
[122] K. Lika, S. Augustine, L. Pecquerie, S. A. L. M. Kooijman, The bijection from data to parameter space with the standard DEB model quantifies the supply–demand spectrum, J. Theor. Biol. 354 (2014) 35–47.
[123] J. Baas, S. A. L. M. Kooijman, Sensitivity of animals to chemical compounds links to metabolic rate, Ecotoxicology 24 (2015) 657–663.
[124] M. Jusup, H. Matsuda, Mathematical modeling of bluefin tuna growth, maturation, and reproduction based on physiological energetics, in: T. Kitagawa, S. Kimura (Eds.), Biology and Ecology of Bluefin Tuna, CRC Press, 2015.
[125] Turtle Taxonomy Working Group (TTWG), Turtles of the world, 2012 update: Annotated checklist of taxonomy, synonymy, distribution, and conservation status, in: A. Rhodin, P. Pritchard, P.C.H.and van Dijk, R. Saumure, K. Buhlmann, J. Iverson, R. Mittermeier (Eds.), Conservation biology of freshwater turtles and tortoises: A compilation project of the IUCN/SSC tortoise and freshwater turtle specialist group. Chelonian Research Monographs No. 5, volume 5, Chelonian Research Foundation, 2012, pp. 000.243–000.328. TTWG: Turtle Taxonomy Working Group [van Dijk, Peter P. and Iverson, John B. and Shaffer, Bradley H. and Bour,Roger and Rhodin, A.G.J.].
[126] N. Thompson, A. Bolten, M. Dodd, S. Epperly, A. Foley, et al., An assessment of the loggerhead turtle population in the western North Atlantic Ocean, in: NOAA Technical Memorandum NMFS-SEFSC (Turtle Expert Working Group), volume 575, 2009, p. 131.
[127] G. H. Parker, The growth of turtles, Proc. Natl. Acad. Sci. U. S. A. 12 (1926) 422–424.
[128] S. F. Hildebrand, C. Hatsel, On the growth, care and behavior of loggerhead turtles in captivity, Proc. Natl. Acad. Sci. U. S. A. 13 (1927) 374–377.
[129] G. Parker, The growth of the loggerhead turtle, Am. Nat. 63 (1929) 367–373.
[130] G. C. Hays, Sea turtles: a review of some key recent discoveries and remaining questions, J. Exp. Mar. Biol. Ecol. 356 (2008) 1–7.
[131] N. Marn, S. A. L. M. Kooijman, M. Jusup, T. Legovic, T. Klanjscek, Inferring physiological energetics of loggerhead turtle (*Caretta caretta*) from existing data using a general metabolic theory, 2016. BioRxiv 070987; doi: dx.doi.org/10.1101/070987.
[132] L. Stokes, J. Wyneken, L. B. Crowder, J. Marsh, The influence of temporal and spatial origin on size and early growth rates in captive loggerhead sea turtles (*Caretta caretta*) in the United States, Herpetol. Conserv. Biol. 1 (2006) 71–80.

[133] M. Godfrey, N. Mrosovsky, Estimating the time between hatching of sea turtles and their emergence from the nest, Chelonian Conserv. Biol. 2 (1997) 581–584.
[134] J. R. Spotila, Sea turtles: A complete guide to their biology, behavior, and conservation, JHU Press, 2004.
[135] J. Braun-McNeill, S. P. Epperly, L. Avens, M. L. Snover, J. C. Taylor, Growth rates of loggerhead sea turtles (*Caretta caretta*) from the western North Atlantic, Herpetol. Conserv. Biol. 3 (2008) 273–281.
[136] J. F. Parham, G. R. Zug, Age and growth of loggerhead sea turtles (*Caretta caretta*) of coastal Georgia: an assessment of skeletochronological age-estimates, Bull. Mar. Sci. 61 (1997) 287–304.
[137] M. L. Snover, Growth and ontogeny of sea turtles using skeletochronology: methods, validation and application to conservation, Ph.D. thesis, Duke University, 2002.
[138] Georgia Sea Turtle Center (GSTC), Frequently asked questions [WWW document], `http://gstc.jekyllisland.com/about-us/faq/`, 2015. Accessed: 15-Aug-2016.
[139] J. Byrd, S. Murphy, A. Von Harten, Morphometric analysis of the northern subpopulation of *Caretta caretta* in South Carolina, USA, Marine Turtle Newsletter 107 (2005) 1–4.
[140] L. Ehrhart, R. Yoder, Marine turtles of Merritt Island National Wildlife Refuge, Kennedy Space Center, Florida, Fla. Mar. Res. Publ. 33 (1978) 25–30.
[141] D. Stoneburner, Body depth: an indicator of morphological variation among nesting groups of adult loggerhead sea turtles (*Caretta caretta*), J. Herpetol. 14 (1980) 205–206.
[142] T. M. Norton, Sea turtle conservation in Georgia and an overview of the Georgia sea turtle center on Jekyll Island, Georgia, Ga. J. Sci. 63 (2005) 208.
[143] M. Tiwari, K. A. Bjorndal, Variation in morphology and reproduction in loggerheads, *Caretta caretta*, nesting in the United States, Brazil, and Greece, Herpetologica 56 (2000) 343–356.
[144] K. J. Reich, K. A. Bjorndal, M. G. Frick, B. E. Witherington, C. Johnson, A. B. Bolten, Polymodal foraging in adult female loggerheads (*Caretta caretta*), Mar. Biol. 157 (2010) 113–121.
[145] G. C. Hays, J. R. Speakman, Reproductive investment and optimum clutch size of loggerhead sea turtles (*Caretta caretta*), J. Anim. Ecol. 60 (1991) 455–462.
[146] J. D. Miller, C. J. Limpus, M. H. Godfrey, Nest site selection, oviposition, eggs, development, hatching, and emergence of loggerhead turtles, in: A. Bolten, B. Witherington (Eds.), The Biology of the Loggerhead Turtle, Smithsonian Institution Press, 2003, p. 125.
[147] L. A. Hawkes, A. C. Broderick, M. H. Godfrey, B. J. Godley, Status of nesting loggerhead turtles *Caretta caretta* at Bald Head Island (North Carolina, USA) after 24 years of intensive monitoring and conservation, Oryx 39 (2005) 65–72.
[148] C. Wabnitz, D. Pauly, Length-weight relationships and additional growth parameters for sea turtles, Fish. Cent. Res. Rep. 16 (2008) 92–101.
[149] L. A. Hawkes, M. J. Witt, A. C. Broderick, J. W. Coker, M. S. Coyne, M. Dodd, M. G. Frick, M. H. Godfrey, D. B. Griffin, S. R. Murphy, et al., Home on the range: spatial ecology of loggerhead turtles in Atlantic waters of the USA, Divers. Distrib. 17 (2011) 624–640.
[150] S. H. Peckham, D. Maldonado-Diaz, Y. Tremblay, R. Ochoa, J. Polovina, G. Balazs, P. H. Dutton, W. J. Nichols, Demographic implications of alternative foraging strategies in juvenile loggerhead turtles *Caretta caretta* of the North Pacific Ocean, Mar. Ecol. Prog. Ser. 425 (2011) 269–280.
[151] J. Pierro, Add_my_pet, *Lepidochelys kempii*, `http://www.bio.vu.nl/thb/deb/deblab/add_my_pet/entries_web//i_results_Lepidochelys_kempii.html`, 2015. Accessed: 15-Aug-2016.
[152] S. A. L. M. Kooijman, Add_my_pet, *Dermochelys coriacea*, `http://www.bio.vu.nl/thb/deb/deblab/add_my_pet/entries_web//i_results_Dermochelys_coriacea.html`, 2015. Accessed: 15-Aug-2016.
[153] K. A. Reid, D. Margaritoulis, J. R. Speakman, Incubation temperature and energy expenditure during development in loggerhead sea turtle embryos, J. Exp. Mar. Biol. Ecol. 378 (2009) 62–68.
[154] L. Woolgar, S. Trocini, N. Mitchell, Key parameters describing temperature-dependent sex determination in the southernmost population of loggerhead sea turtles, J. Exp. Mar. Biol. Ecol. 449 (2013) 77–84.
[155] J. E. Kraemer, S. H. Bennett, Utilization of posthatching yolk in loggerhead sea turtles, *Caretta caretta*, Copeia 1981 (1981) 406–411.
[156] L. Pecquerie, P. Petitgas, S. A. L. M. Kooijman, Modeling fish growth and reproduction in the context of the dynamic energy budget theory to predict environmental impact on anchovy spawning duration, J. Sea Res. 62

(2009) 93–105.
[157] M. Jusup, T. Klanjscek, H. Matsuda, S. A. L. M. Kooijman, A full lifecycle bioenergetic model for bluefin tuna, PLoS ONE 6 (2011) e21903.
[158] R. Fablet, L. Pecquerie, H. De Pontual, H. Høie, R. Millner, H. Mosegaard, S. A. L. M. Kooijman, Shedding light on fish otolith biomineralization using a bioenergetic approach, PLoS ONE 6 (2011) e27055.
[159] L. Pecquerie, R. Fablet, H. De Pontual, S. Bonhommeau, M. Alunno-Bruscia, P. Petitgas, S. A. L. M. Kooijman, Reconstructing individual food and growth histories from biogenic carbonates, Mar. Ecol. Prog. Ser. 447 (2012) 151–164.
[160] T. Jager, Some good reasons to ban ECx and related concepts in ecotoxicology, Environ. Sci. Technol. 45 (2011) 8180–8181.
[161] Current approaches in the statistical analysis of ecotoxicity data: a guidance to application, Technical Report 54, Organisation for Economic Co-operation and Development, 2 rue Andr-Pascal, 75775 Paris Cedex 16, France, 2006.
[162] J. Baas, T. Jager, S. A. L. M. Kooijman, A review of DEB theory in assessing toxic effects of mixtures, Sci. Total Environ. 408 (2010) 3740–3745.
[163] T. Jager, T. Vandenbrouck, J. Baas, W. M. De Coen, S. A. L. M. Kooijman, A biology-based approach for mixture toxicity of multiple endpoints over the life cycle, Ecotoxicology 19 (2010) 351–361.
[164] T. Jager, A. Barsi, N. T. Hamda, B. T. Martin, E. I. Zimmer, V. Ducrot, Dynamic energy budgets in population ecotoxicology: Applications and outlook, Ecol. Model. 280 (2014) 140–147.
[165] Debtox information: Making sense of ecotoxicity test results [WWW document], `http://www.debtox.info/papers_debtox.html`, 2011. Accessed: 15-Aug-2016.
[166] T. Klanjscek, R. M. Nisbet, H. Caswell, M. G. Neubert, A model for energetics and bioaccumulation in marine mammals with applications to the right whale, Ecol. Appl. 17 (2007) 2233–2250.
[167] T. Jager, B. T. Martin, E. I. Zimmer, DEBkiss or the quest for the simplest generic model of animal life history, J. Theor. Biol. 328 (2013) 9–18.
[168] T. Klanjscek, H. Caswell, M. G. Neubert, R. M. Nisbet, Integrating dynamic energy budgets into matrix population models, Ecol. Model. 196 (2006) 407–420.
[169] I. M. van Leeuwen, J. Vera, O. Wolkenhauer, Dynamic energy budget approaches for modelling organismal ageing, Phil. Trans. R. Soc. B 365 (2010) 3443–3454.
[170] H. Caswell, Matrix population models, Wiley Online Library, 2001.
[171] M. Kot, Elements of mathematical ecology, Cambridge University Press, 2001.
[172] C. Bacher, A. Gangnery, Use of dynamic energy budget and individual based models to simulate the dynamics of cultivated oyster populations, J. Sea Res. 56 (2006) 140–155.
[173] T. Klanjscek, Dynamic energy budgets and bioaccumulation: a model for marine mammals and marine mammal populations, Ph.D. thesis, Massachusetts Institute of Technology and Woods Hole Oceanographic Institution, 2006.
[174] B. T. Martin, E. I. Zimmer, V. Grimm, T. Jager, Dynamic Energy Budget theory meets individual-based modelling: a generic and accessible implementation, Methods Ecol. Evol. 3 (2012) 445–449.
[175] B. T. Martin, T. Jager, R. M. Nisbet, T. G. Preuss, V. Grimm, Predicting population dynamics from the properties of individuals: a cross-level test of Dynamic Energy Budget theory, Am. Nat. 181 (2013) 506–519.
[176] R. M. Nisbet, E. McCauley, L. R. Johnson, Dynamic energy budget theory and population ecology: lessons from Daphnia, Phil. Trans. R. Soc. B 365 (2010) 3541–3552.
[177] B. Ananthasubramaniam, E. McCauley, K. A. Gust, A. J. Kennedy, E. B. Muller, E. J. Perkins, R. M. Nisbet, Relating suborganismal processes to ecotoxicological and population level endpoints using a bioenergetic model, Ecol. Appl. 25 (2015) 1691–1710.
[178] T. Klanjscek, R. M. Nisbet, J. H. Priester, P. A. Holden, Modeling physiological processes that relate toxicant exposure and bacterial population dynamics, PLoS ONE 7 (2012) e26955.
[179] T. Klanjscek, R. M. Nisbet, J. H. Priester, P. A. Holden, Dynamic energy budget approach to modeling mechanisms of CdSe quantum dot toxicity, Ecotoxicology 22 (2013) 319–330.
[180] M. N. Berberan-Santos, Greens function method and the first-order linear differential equation, J. Math. Chem. 48 (2010) 175–178.